Non-Terrestrial Networks for UAVs: Base Station Service Provisioning Schemes with Antenna Tilt

Seongjun Kim, Minsu Kim, Jong Yeol Ryu, *Member, IEEE*,
Jemin Lee, *Member, IEEE*, and Tony Q. S. Quek, *Fellow, IEEE*

Abstract—By focusing on unmanned aerial vehicle (UAV) communications in non-terrestrial networks (NTNs), this paper provides a guideline on the appropriate base station (BS) service provisioning scheme with considering the antenna tilt angle of BS. Specifically, two service provisioning schemes are considered including the inclusive-service BS (IS-BS) scheme, which makes BSs serve both ground users (GUs) and aerial users (AUs) (i.e., UAVs) simultaneously, and the exclusive-service BS (ES-BS) scheme, which has BSs for GUs and BSs for AUs. By considering the antenna tilt angle-based channel gain, we derive the network outage probability for both IS-BS and ES-BS schemes, and show the existence of the optimal tilt angle that minimizes the network outage probability after analyzing the conflict impact of the antenna tilt angle. We also analyze the impact of various network parameters, including the ratio of GUs to total users and densities of total and interfering BSs, on the network outage probability. Finally, we analytically and numerically show in which environments each service provisioning scheme can be superior to the other one.

Index Terms—Non-terrestrial network, unmanned aerial vehicle, antenna tilt angle, line-of-sight (LoS) probability, outage probability

I. INTRODUCTION

Due to an increasing demand for novel and high-quality mobile services, it becomes more difficult to provide reliable communications by the existing terrestrial networks only, up to the level required by future mobile services. To address these issues, non-terrestrial networks (NTNs) have been considered as a promising solution to complement terrestrial networks by providing ubiquitous and global connectivity [2], [3]. Conventional 2D ground space in terrestrial networks is now expanded to 3D aerial space in NTNs with supporting communications for unmanned aerial vehicles (UAVs), high altitude platform

systems (HAPS), and satellites [4]. Among them, UAV communications have been in the spotlight because UAVs have more flexible mobility and can locate closer to ground users and base stations (BSs) in terrestrial networks, compared to HAPS and satellites. Therefore, many applications and services based on UAV communications have appeared such as working as a relay in hotspot and a data collector in large-scale networks [5]–[7]. However, the integration of UAVs into existing terrestrial networks brings a lot of challenges such as resource and interference management since UAV communications usually use the frequency band as well as BSs of terrestrial networks.

In this context, many works have been presented for reliable UAV communications. At the beginning of studies, the wireless channel modeling of UAV networks has been studied in [8]–[11], which is different from that of terrestrial networks. Specifically, according to the height of the UAV, the distance-dependent path loss model for the cellular-to-UAV channel and the line-of-sight (LoS) probability between the UAV and the ground device were modeled in [8], [9] and [10], [11], respectively. Based on the wireless channel modeling of UAV networks, the works in [12]–[19] studied to present the optimal location of UAVs for various environments and applications. The deployment and the power allocation for the UAV jointly optimized to minimize the outage probability in [12], [13]. The height of the UAV and the antenna beamwidth jointly optimized to maximize the data rate [14] and the coverage probability [15]. The joint optimization of the UAV trajectory and the spectrum allocation were considered to maximize the throughput [16] and minimize the mission completion time [17]. The outage probability was presented by considering the effect of the UAV height and the channel environment in [18].

In [19], multi-layer aerial networks have been considered and designed optimally to maximize the successful transmission probability and the area spectral efficiency. However, the works in [13], [14], [16], [17] made a strict assumption that UAV-to-ground communications channels are dominated by LoS links only without considering the location-dependent probability of having LoS links. Furthermore, all of those aforementioned works did not consider a BS antenna tilt angle, which significantly affects the communication performance between the ground BS and the UAV. Especially, the antenna tilt angle of the ground BS has been conventionally designed for ground devices only, so the UAV can actually receive the signal from these BSs with considerably small power [20],

[21].

To overcome these issues, the efficient design of the BS antenna tilt angle for UAV communications has been considered in recent works [22]–[28]. The vertical antenna gain was considered for analyzing the successful transmission probability of UAV communications in [22]. The BS antenna tilt angle was optimized to maximize the coverage probability according to the heights of the UAV and the BS in [23], [24], and also to maximize the successful content delivery probability in massive multiple-input multiple-output (MIMO) systems in [25]. The BS association probability and signal-to-interference-plus-noise ratios (SINRs) were studied for two different association policies such as nearest-distance based and maximum-power based associations by considering the antenna gain, determined by the tilt angle in [26]. The handover rate as well as the coverage probability were analyzed by considering the practical antenna configuration [27] and also for the coordinated multi-point (CoMP) transmission [28].

However, the aforementioned works considered limited scenarios and parameters of UAV networks in the design of the antenna tilt angle. For instance, in [22], [27], [28], a simple UAV network, where ground users (GUs) do not exist, was considered in spite of using ground BSs. In [22]–[28], they considered either the down tilt angle or the up tilt angle although both should be considered to support aerial users (AUs) together with GUs. In [23]–[25], [28], a simple constant power gain model was used for the antenna main lobe although it can be changed according to the BS antenna tilt angle as well as the elevation angle of the communications link [29]. Furthermore, only the *inclusive-service BS (IS-BS) scheme* that makes each BS serves both GUs and AUs was explored as in [22], [23], [25]. However, the *exclusive-service BS (ES-BS) scheme* that makes BSs serve GUs or AUs exclusively might be a better scheme for certain UAV network environments. Therefore, in existing works, it failed to present or analyze the performance of UAV communications with more realistic tilt angle-based antenna gains as well as existing both GUs and AUs in the networks.

Therefore, in this paper, we provide a framework to explore an appropriate BS service provisioning scheme to support both GUs and AUs with considering the tile angle-based antenna gain. First, the network outage probabilities of the *ES-BS scheme* as well as the *IS-BS scheme* are analyzed. We then explore how the optimal antenna title angles of BSs that minimize the network outage probability are determined for different service provisioning schemes as well as different types of BSs. The impact of various network parameters such as the spatial densities of total BSs and interfering BSs on the performance of service provisioning schemes are also discussed. The main contributions of this paper are summarized as follows.

- We newly derive the network outage probability for two BS service provisioning schemes, i.e., IS-BS and ES-BS schemes, by considering the tilt angle-based antenna gain in both general environment (where the interference exists) and noise-limited environment.
- We analytically show that changing the antenna tilt angle gives conflicting impacts on the network outage proba-

bility. Specifically, as the absolute value of the tilt angle decreases, the service area with the main lobe becomes wider (i.e., positive impact), but the link distance between the serving BS and the user increases (i.e., negative impact). From these results, we show that there exists the optimal BS antenna tilt angle that minimizes the network outage probability.

- We show the impact of various network parameters on the optimal antenna tilt angle that minimizes the network outage probability including the BS height, the UAV height, the ratio of GU, as well as densities of the total BSs and the interfering BSs. For instance, we show that the optimal antenna tilt angle increases as the ratio of GUs increases, and the absolute value of the tilt angle increases, as the total BS density increases.
- We also explore which service provisioning scheme can be better in terms of the network outage probability in various environments. Specifically, in the noise-limited environment, we *analytically* show the superiority of the ES-BS scheme to the IS-BS scheme for high BS density regime. In the general environment, we numerically show the superiority of the IS-BS scheme for low interfering BS density regime and that of the ES-BS scheme for high interfering BS density regime.

The rest of this paper is organized as follows. In Section II, we represent the BS service provisioning schemes to serve both types of users and describe the channel model and the BS antenna power gain, which is affected by the BS antenna tilt angle. We then describe the BS association rule. In Section III, we derive the network outage probability for two service provisioning schemes in the general environment and the noise-limited environment, respectively. In Section IV, we evaluate the network outage probability according to the various network design parameters. We then compare the communication performance of the IS-BS scheme and that of the ES-BS scheme for network parameters. Finally, conclusions are presented in V.

Notation: The notation used throughout the paper is listed in Table I.

II. SYSTEM MODEL

In this section, we introduce the non-terrestrial network model by mainly focusing on UAV networks. Moreover, we describe the antenna power gain and the BS association rules.

A. Network Model

We consider a NTN for UAVs, where BSs, ground users (GUs), and aerial users (AUs) (i.e., UAVs) are randomly distributed in the spatial domain. The locations of users are modeled by homogeneous Poisson point process (HPPP) $\Phi_{\mathrm{U},i}$ with density λ_i, where $i \in \{\mathrm{G}, \mathrm{A}\}$ denotes the type of users, i.e., $i = \mathrm{G}$ for GUs and $i = \mathrm{A}$ for AUs.[1]

---

[1]Note that we can also assume AUs are distributed according to Matérn Hardcore Point Processes (MHCPP) with density λ_{A} that considers the minimum safety horizontal distance, $d_{\min}$, between any two AUs like the ones in [30], [31]. However, the performance analysis and the results of this work will be the same as only the density of AUs affects the performance, not the distribution as the downlink is considered.

TABLE I
NOTATIONS USED THROUGHOUT THE PAPER.

Notation	Definition
$i \in \{G, A\}$	User type index for GUs ($i = G$) and AUs ($i = A$)
$l \in \{O, G, A\}$	BS type index for IS-BS ($l = O$), GBS ($l = G$) and ABS ($l = A$)
$v \in \{L, N\}$	Index for the LoS environment ($v = L$) and the non-line-of-sight (NLoS) environment ($v = N$)
$s \in \{IS, ES\}$	Index for the IS-BS scheme ($s = IS$) and the ES-BS scheme ($s = ES$)
$r_{k, \mathbf{x}}$	Horizontal distance between the kth user and the BS located at $\mathbf{x}$
h_B / h_k	Height of the BS and the kth user
$\Omega_{k, \mathbf{x}}$	Channel fading between the kth user and the BS
$\theta_{t,O}^{IS}$ / $\theta_{t,G}^{ES}$, $\theta_{t,A}^{ES}$	Antenna tilt angle of the IS-BS / Antenna tilt angles of GBS and ABS in the ES-BS scheme.
P_t	Transmission power of the BS
γ_t	Target SINR/SNR
$l_v(r_{k, \mathbf{x}})$	Path loss between the kth user and the BS
$p_L(r_{k, \mathbf{x}})$ / $p_N(r_{k, \mathbf{x}})$	LoS and NLoS probability for given $r_{k, \mathbf{x}}$
$G(r_{k, \mathbf{x}}, \theta_t)$	Antenna power gain for given $r_{k, \mathbf{x}}$ and θ_t
$r_G^{lb}(\theta_t)$ / $r_A^{lb}(\theta_t)$	Lower bound of the horizontal distance that the user is served by main lobe for GUs and AUs
$r_G^{ub}(\theta_t)$ / $r_A^{ub}(\theta_t)$	Upper bound of the horizontal distance that the user is served by main lobe for GUs and AUs
$f_{r_{k, \mathbf{x}_\tau}}^{s, a}(r)$	PDF of the horizontal distance between the kth user and the serving BS for given scheme s and association rule a
ρ_i	Ratio of i-type users to total users
$\rho_{B,i}$	Ratio of BSs for i-type user to total BSs
λ_B / λ_I	Densities of total BS and total interfering BS
$\lambda_{B,i}^s$	BS density for i-type user in scheme s
$\lambda_{I,O}^{IS}$ / $\lambda_{I,G}^{ES}$, $\lambda_{I,A}^{ES}$	Density of interfering IS-BS / Densities of interfering GBS and ABS in the ES-BS scheme.
I_O^{IS} / I_G^{ES}, I_A^{ES}	Interference from IS-BSs / Interference from GBSs and ABSs in the ES-BS scheme.
$\mathcal{P}_{no}^s(\theta_{t,G}^s, \theta_{t,A}^s)$	Network outage probability in the general environment for given s
$\hat{\mathcal{P}}_{no}^s(\theta_{t,G}^s, \theta_{t,A}^s)$	Network outage probability in the noise-limited environment for given s
$\tilde{\mathcal{P}}_{no}^s(\theta_{t,G}^s, \theta_{t,A}^s)$	Network outage probability with simplified antenna gain model for given s.

The height of the kth user is h_k, where $h_k = h_G$ for $k \in \mathcal{U}_G$ and $h_k = h_A$ for $k \in \mathcal{U}_A$. Here $\mathcal{U}_G$ and $\mathcal{U}_A$ are the user index sets of GUs and AUs, respectively.

In this paper, as shown in Figure 1, we consider the two types of BS service provisioning schemes as follows.

- *Inclusive-service BS (IS-BS) scheme*: In this scheme, BSs serve both GUs and AUs simultaneously. Hence, the antenna tilt angle of the BS has to be designed to serve both GUs and AUs efficiently. The locations of BSs are modeled by HPPP $\Phi_{B,O}$ with density λ_B. Since there is only one type of BS, the BS density for GUs, $\lambda_{B,G}^{IS}$, and the BS density for AUs, $\lambda_{B,A}^{IS}$, are the same as the total BS density (i.e., $\lambda_{B,G}^{IS} = \lambda_{B,A}^{IS} = \lambda_B$). Note that this scheme is the one, generally used in prior works such as [22], [23], [25].
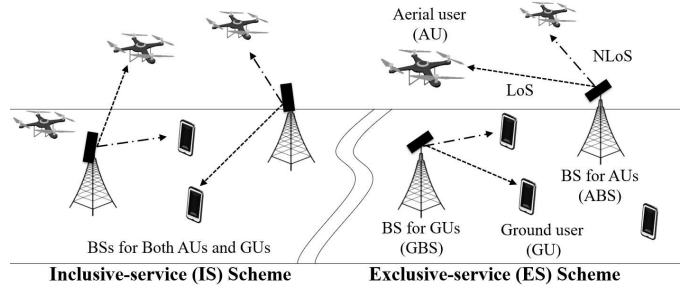

Fig. 1. Examples of NTN for UAVs with randomly distributed BSs, GUs, and AUs.

- *Exclusive-service BS (ES-BS) scheme*: In this scheme, BSs are divided into two groups: 1) a BS for GUs (BS for GUs (GBS)) and 2) a BS for AUs (BS for AUs (ABS)). The GBSs and ABSs exclusively serve GUs and AUs, respectively. Therefore, the antenna tilt angles of GBSs and ABSs need to be designed respectively to serve aimed users efficiently. We assume the distributions of GBSs and ABSs also follow HPPPs, $\Phi_{B,G}$ and $\Phi_{B,A}$, with densities $\lambda_{B,G}^{ES} = \rho_{B,G}\lambda_B$ and $\lambda_{B,A}^{ES} = (1 - \rho_{B,G})\lambda_B$, respectively, where $\rho_{B,G}$ is the portion of GBSs among all BSs.

Regardless of BS types, for all BSs, the antenna height is h_B and the transmission power is P_t.

B. Channel Model

In UAV communications, both LoS and NLoS environments can be considered for the links between a BS and a GU as well as between a BS and an AU. The probability of forming LoS link between the BS at $\mathbf{x} = (x_B, y_B, h_B)$ and the kth user at (x_k, y_k, h_k) is given by [32][2]

$$p_L(r_{k, \mathbf{x}}) = \left\{1 - \frac{\sqrt{2\pi}\xi}{|h_k - h_B|}\left|Q\left(\frac{h_k}{\xi}\right) - Q\left(\frac{h_B}{\xi}\right)\right|\right\}^{r_{k, \mathbf{x}}\sqrt{\mu\nu}},$$
(1)

where $Q(x) = \int_x^\infty \frac{1}{\sqrt{2\pi}}\exp(-\frac{t^2}{2})dt$ is the Q-function and the horizontal distance between the BS and the kth user is given by $r_{k, \mathbf{x}} = \sqrt{(x_k - x_B)^2 + (y_k - y_B)^2}$. Here, μ, ν and ξ are environment parameters determined by the density and the height of obstacles. Since the NLoS environment is a complementary event of the LoS environment, the NLoS probability between the BS and the kth user is given by $p_N(r_{k, \mathbf{x}}) = 1 - p_L(r_{k, \mathbf{x}})$.

Based on the LoS probability, we consider different path loss exponents and channel fading models for LoS and NLoS links. The path loss exponent for LoS and NLoS links are denoted by α_L and α_N, respectively. The channel fading is modeled by Nakagami-m fading, so the distribution of the channel gain is given by

$$f_{\Omega_v}(x) = \frac{m_v^{m_v}}{\Gamma(m_v)}x^{m_v - 1}\exp(-m_v x), \quad x > 0, \quad (2)$$

[2]The LoS probability is also defined differently in [10]. However, it is determined by the elevation angle between the transmitter and the receiver, not by the link distance.
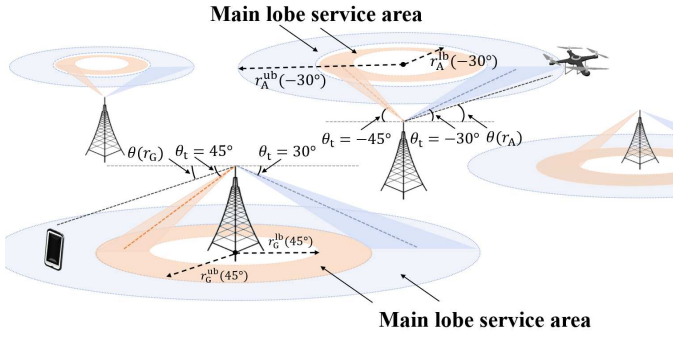
Fig. 2. Examples of antenna radiation patterns for different antenna tilt angles.

where $\Gamma(x) = \int_0^\infty t^{x-1}e^{-t}dt$ and $v \in \{L, N\}$ is the channel environment, i.e., $v = L$ for LoS links and $v = N$ for NLoS links. In addition, we assume that $m_L > 1$, and $m_N = 1$, which means Rayleigh fading, i.e., $\Omega_N \sim \exp(1)$. From (2), we denote the channel fading between the kth user and the BS as

$$\Omega_{k,\mathbf{x}} = \begin{cases} \Omega_L, & \text{with probability } p_L(r_{k,\mathbf{x}}) \\ \Omega_N, & \text{otherwise} \end{cases}. \quad (3)$$

C. Vertical Antenna Gain

The antenna power gain of the BS is determined by two types of power gains: horizontal and vertical directional antenna gains. We consider an omnidirectional antenna in the horizontal direction, so the horizontal directional antenna gain remains constant regardless of the direction of the antenna. Therefore, we assume the horizontal directional antenna gain is equal to a unit gain [33]. In this paper, we focus on the design of the vertical antenna tilt angle for AUs as well as GUs, and we consider the directional antenna in the vertical direction. As shown in Fig. 2, the vertical directional antenna gain is determined by the vertical antenna tilt angle, $-90° < \theta_t < 90°$, which is the angle tilted upward or downward relative to the horizontal plane.[3] Here, we define that the BS antenna tilt angle is a negative value when the BS antenna tilt angle is up-tilted, i.e., tilting upwards with respect to the horizontal plane of the BS antenna. On the other hand, the BS antenna tilt angle is defined as a positive value when the BS antenna tilt angle is down-tilted, i.e., tilting downwards with respect to the horizontal plane of the BS antenna. Based on the 3rd generation partnership project (3GPP) specification [29], for given $r_{k,\mathbf{x}}$, the BS antenna power gain $G(r_{k,\mathbf{x}}, \theta_t)$ can be represented by a function of the tilt angle as

$$G(r_{k,\mathbf{x}}, \theta_t) = 10^{-\min\left(12\left(\frac{\theta(r_{k,\mathbf{x}})+\theta_t}{\theta_{3dB}}\right)^2, \eta\right)/10}, \quad (4)$$

[3]Note that there are two types of tilting methods [34]: mechanical tilting and electrical tilting. The mechanical tilting rotates the antenna of the BS physically. On the other hand, the electrical tilting applies an overall phase shift to all antenna elements in the array. In this paper, we consider the electrical tilting method to analyze the communication performance mathematically.

where $\theta_{3dB} = 10°$ is the 3dB beamwidth and η is the minimum power leaking to the side lobe besides the main lobe, which is commonly 20dB. In (4), $\theta(r_{k,\mathbf{x}})$ is the elevation angle between the BS antenna and the kth user, which is given by

$$\theta(r_{k,\mathbf{x}}) = \frac{180}{\pi}\arctan\left(\frac{h_k - h_B}{r_{k,\mathbf{x}}}\right), \quad (5)$$

where $h_k - h_B$ is the height difference between the BS and the kth user. In this work, without loss of generality, we assume that the height of AUs is higher than that of BSs (i.e., $h_A - h_B > 0$), while the height of GUs is lower than that of BSs (i.e., $h_G - h_B < 0$). From (4), for given θ_t, the user can be served with the main lobe when $12\left(\frac{\theta(r_{k,\mathbf{x}})+\theta_t}{\theta_{3dB}}\right)^2 \geq \eta$. Here, we define the boundary of horizontal distance between a BS and the kth user that the user is served by the main lobe as $r_k^{lb}(\theta_t) \leq r_{k,\mathbf{x}} \leq r_k^{ub}(\theta_t)$, where $r_k^{lb}(\theta_t)$ and $r_k^{ub}(\theta_t)$ are the lower and upper boundaries. Since all GUs and all AUs have the same height, h_G and h_A, respectively, the boundaries are determined by the user types not user's specific location, i.e. $r_k^{ub}(\theta_t) = r_i^{ub}(\theta_t)$ and $r_k^{lb}(\theta_t) = r_i^{lb}(\theta_t)$ for $k \in \mathcal{U}_i$, and given as follows

$$r_G^{lb}(\theta_t) = \begin{cases} \dfrac{h_G - h_B}{\tan\left\{\frac{\pi}{180}(-\theta_t - \theta_{th})\right\}}, & \theta_t > -\theta_{th} \\ \infty, & \text{otherwise} \end{cases}, \quad (6)$$

$$r_G^{ub}(\theta_t) = \begin{cases} \dfrac{h_G - h_B}{\tan\left\{\frac{\pi}{180}(-\theta_t + \theta_{th})\right\}}, & \theta_t > \theta_{th} \\ \infty, & \text{otherwise} \end{cases}, \quad (7)$$

$$r_A^{lb}(\theta_t) = \begin{cases} \dfrac{h_A - h_B}{\tan\left\{\frac{\pi}{180}(-\theta_t + \theta_{th})\right\}}, & \theta_t < \theta_{th} \\ \infty, & \text{otherwise} \end{cases} \quad (8)$$

$$r_A^{ub}(\theta_t) = \begin{cases} \dfrac{h_A - h_B}{\tan\left\{\frac{\pi}{180}(-\theta_t - \theta_{th})\right\}}, & \theta_t < -\theta_{th} \\ \infty, & \text{otherwise} \end{cases}, \quad (9)$$

where $\theta_{th} = \theta_{3dB}\sqrt{\eta/12}$. In (6)-(9), the boundaries $r_i^{ub}(\theta_t)$ and $r_i^{lb}(\theta_t)$ are defined to be positive when θ_t satisfies each conditions. For the convenience of analysis, we rewrite $G(r_{k,\mathbf{x}}, \theta_t)$ in (4) according to the boundaries in (6)-(9) as

$$G(r_{k,\mathbf{x}}, \theta_t) = \begin{cases} G_1(r_{k,\mathbf{x}}, \theta_t), & b_{k,1}(\theta_t) < r_{k,\mathbf{x}} < b_{k,2}(\theta_t) \\ G_2(r_{k,\mathbf{x}}, \theta_t), & b_{k,2}(\theta_t) \leq r_{k,\mathbf{x}} \leq b_{k,3}(\theta_t) \\ G_3(r_{k,\mathbf{x}}, \theta_t), & b_{k,3}(\theta_t) < r_{k,\mathbf{x}} < b_{k,4}(\theta_t) \end{cases} \quad (10)$$

where $b_{k,1}(\theta_t) = 0$, $b_{k,2}(\theta_t) = r_k^{lb}(\theta_t)$, $b_{k,3}(\theta_t) = r_k^{ub}(\theta_t)$, and $b_{k,4}(\theta_t) = \infty$. In (10), $G_1(r_{k,\mathbf{x}}, \theta_t) = G_3(r_{k,\mathbf{x}}, \theta_t) = 10^{-\eta/10}$ is the antenna side lobe gain and $G_2(r_{k,\mathbf{x}}, \theta_t)$ is the antenna main lobe gain, which is given by

$$G_2(r_{k,\mathbf{x}}, \theta_t) = 10^{-1.2\left\{\frac{\theta(r_{k,\mathbf{x}})+\theta_t}{\theta_{3dB}}\right\}^2}. \quad (11)$$

From (11), we can see that $G_2(r_{k,\mathbf{x}}, \theta_t)$ is an increasing function of θ_t for $-\theta_{th} < \theta_t \leq -\theta(r_{k,\mathbf{x}})$, and $G_2(r_{k,\mathbf{x}}, \theta_t)$ is a decreasing function of θ_t for $-\theta(r_{k,\mathbf{x}}) \leq \theta_t < \theta_{th}$. This is because as the antenna tilt angle θ_t approaches the elevation angle between the BS and the user, the effect of the main lobe

$$\mathbb{P}\left[X_k^{vj} \leq r, \mathbf{x}_\tau \in \Phi_{\mathrm{B},l}^{vj} \mid a = \mathrm{sa}\right] \overset{(a)}{=} \int_{b_{k,j}(\theta_\mathrm{t})}^r f_{X_k^{vj}}^s(x) \prod_{\substack{j_o \in \mathcal{J}, v_o \in \{\mathrm{L,N}\}, \\ (j_o,v_o) \neq (j,v)}} \mathbb{P}\left[G_j(x,\theta_\mathrm{t})(x^2 + h_k^2)^{-\frac{\alpha_v}{2}} \geq G_{j_o}\left(X_k^{v_oj_o}, \theta_\mathrm{t}\right)\left((X_k^{v_oj_o})^2 + h_k^2\right)^{-\frac{\alpha_{v_o}}{2}}\right] dx. \tag{16}$$

becomes dominant and it is maximized when the antenna tilt angle is equal to the elevation angle (i.e., $\theta_\mathrm{t} = -\theta(r_{k,\mathbf{x}})$).

D. BS Association Rule

In conventional networks, the BS association is determined by the mean channel fading gain and the distance-dependent path loss, considering the LoS probability [35]. However, in more realistic UAV networks, the antenna gain $G(r_{k,\mathbf{x}}, \theta_\mathrm{t})$ affected by the horizontal distance between the serving BS and the kth user should also be considered in the BS association.

To analyze BS association rules, we first denote BSs which belong to $\Phi_{\mathrm{B},l}, l \in \{\mathrm{O,G,A}\}$, forming LoS and NLoS links as $\Phi_{\mathrm{B},l}^\mathrm{L}$ and $\Phi_{\mathrm{B},l}^\mathrm{N}$, respectively. We then divide each of $\Phi_{\mathrm{B},l}^\mathrm{L}$ and $\Phi_{\mathrm{B},l}^\mathrm{N}$ into three groups according to the BS antenna power gain $G(r_{k,\mathbf{x}}, \theta_\mathrm{t})$ in (10) as

$$\Phi_{\mathrm{B},l}^{vj} = \begin{cases} \Phi_{\mathrm{B},l}^{v1}, & b_{k,1}(\theta_\mathrm{t}) < r_{k,\mathbf{x}} < b_{k,2}(\theta_\mathrm{t}) \\ \Phi_{\mathrm{B},l}^{v2}, & b_{k,2}(\theta_\mathrm{t}) \leq r_{k,\mathbf{x}} \leq b_{k,3}(\theta_\mathrm{t}) \\ \Phi_{\mathrm{B},l}^{v3}, & b_{k,3}(\theta_\mathrm{t}) < r_{k,\mathbf{x}} < b_{k,4}(\theta_\mathrm{t}) \end{cases}, \; v \in \{\mathrm{L,N}\}, \tag{12}$$

where $j \in \mathcal{J}$ is the index of BS groups which is determined by $r_{k,\mathbf{x}}$, and $\mathcal{J} = \{1,2,3\}$. Note that from (10) and (12), we know that BSs in $\Phi_{\mathrm{B},l}^{v1}$ or $\Phi_{\mathrm{B},l}^{v3}$ transmit with the antenna side lobe gain, and BSs in $\Phi_{\mathrm{B},l}^{v2}$ transmit with the antenna main lobe gain. First of all, we examine the distribution of the distance between the user and the BS in $\Phi_{\mathrm{B},l}^{vj}$. The horizontal distance to the nearest BS among the BSs in $\Phi_{\mathrm{B},l}^{vj}$ is denoted by X_k^{vj}. Here, depending on the LoS probability, the density function of $\Phi_{\mathrm{B},l}^{vj}$ is given by $2\pi\lambda_{\mathrm{B},k}^s t p_v(t)$. Therefore, for BSs in $\Phi_{\mathrm{B},l}^{vj}$, the complementary cumulative distribution function (CCDF) of X_k^{vj} can be obtained as

$$\bar{F}_{X_k^{vj}}^s(x) = \mathbb{P}\left[X_k^{vj} \geq x\right] \overset{(a)}{=} \exp\left\{-2\pi\lambda_{\mathrm{B},k}^s \int_{b_{k,j}(\theta_\mathrm{t})}^{u_{k,j}(x,\theta_\mathrm{t})} t p_v(t) dt\right\}, \tag{13}$$

where (a) is from the void probability [36] and $u_{k,j}(x,\theta_\mathrm{t})$ is given as $u_{k,1}(x,\theta_\mathrm{t}) = \min(x, b_{k,j+1}(\theta_\mathrm{t}))$ if $j = 1$, $u_{k,j}(x,\theta_\mathrm{t}) = \max(x, b_{k,j}(\theta_\mathrm{t}))$, otherwise. $\lambda_{\mathrm{B},k}^s$ is the density of BSs that can serve the kth user, i.e., $\lambda_{\mathrm{B},k}^s = \lambda_{\mathrm{B},i}^s$ when $k \in \mathcal{U}_i$. Here, $s \in \{\mathrm{IS,ES}\}$ is the index of the BS service provisioning scheme. By differentiating (13), we can obtain the probability distribution function (PDF) of X_k^{vj} as

$$f_{X_k^{vj}}^s(x) = 2\pi\lambda_{\mathrm{B},k}^s x p_v(x) \exp\left\{-2\pi\lambda_{\mathrm{B},k}^s \int_{b_{k,j}(\theta_\mathrm{t})}^x t p_v(t) dt\right\}, \tag{14}$$

where $f_{X_k^{vj}}^s(x) = 0$ if $x \leq b_{k,j}(\theta_\mathrm{t})$.

We denote $a \in \{\mathrm{na, sa}\}$ as the index of the BS association criterion. Here, $a = \mathrm{na}$ and $a = \mathrm{sa}$ indicate the nearest BS association rule and the strongest BS association rule, respectively.

1) Nearest BS Association Rule: In the nearest BS association rule ($a = \mathrm{na}$), the horizontal distance between the kth user and the serving BS is smallest. Therefore, the probability that the serving BS exists in $\Phi_{\mathrm{B},l}^{vj}$, and the horizontal distance between the serving BS and the kth user is smaller than r is given by

$$\mathbb{P}\left[X_k^{vj} \leq r, \mathbf{x}_\tau \in \Phi_{\mathrm{B},l}^{vj} \mid a = \mathrm{na}\right]$$
$$\overset{(a)}{=} \int_{b_{k,j}(\theta_\mathrm{t})}^r f_{X_k^{vj}}^s(x) \prod_{\substack{j_o \in \mathcal{J}, v_o \in \{\mathrm{L,N}\}, \\ (j_o,v_o) \neq (j,v)}} \mathbb{P}\left[x \leq X_k^{v_oj_o}\right] dx.$$
$$= \int_{b_{k,j}(\theta_\mathrm{t})}^r f_{X_k^{vj}}^s(x) \prod_{\substack{j_o \in \mathcal{J}, v_o \in \{\mathrm{L,N}\}, \\ (j_o,v_o) \neq (j,v)}} \bar{F}_{X_k^{v_oj_o}}^s(x) dx, \tag{15}$$

where $\mathbf{x}_\tau$ denotes the location of the serving BS and (a) is from the fact that for given j and v, the horizontal distance between the serving BS and the user is shorter than all other candidates.

2) Strongest BS Association Rule: In the strongest BS association rule ($a = \mathrm{s}$), the main link has the strongest average received power. The probability that the serving BS exists in $\Phi_{\mathrm{B},l}^{vj}$ and the horizontal distance between the serving BS and the kth user is smaller than r is given in (16), shown at the top of this page. In (16), (a) is from the fact that for given j and v, the average power of the serving BS should be greater than all other candidates.

From (15) and (16), given $a \in \{\mathrm{na, sa}\}$, we can obtain the association probability $\mathcal{A}_{vj}^a$ as

$$\mathcal{A}_{vj}^a = \mathbb{P}\left[X_k^{vj} \leq b_{k,j+1}(\theta_\mathrm{t}), \mathbf{x}_\tau \in \Phi_{\mathrm{B},l}^{vj} \mid a\right]. \tag{17}$$

Therefore, when the kth user is associated with a BS in j-group under the channel environment v, the cumulative distribution function (CDF) of the horizontal distance between the BS and the user, $r_{k,\mathbf{x}_\tau}^{vj}$, is given by

$$F_{r_{k,\mathbf{x}_\tau}^{vj}}^{s,a}(r) = \mathbb{P}\left[X_k^{vj} \leq r, \mathbf{x}_\tau \in \Phi_{\mathrm{B},l}^{vj} \mid a\right] / \mathcal{A}_{vj}^a. \tag{18}$$

By differentiating (18), we can obtain the PDF of $r_{k,\mathbf{x}_\tau}^{vj}$

$$f_{r_{k,\mathbf{x}_\tau}^{vj}}^{s,a}(r) = \begin{cases} \dfrac{2\pi\lambda_{\mathrm{B},k}^s x p_v(x)}{\mathcal{A}_{vj}^{\mathrm{na}}} \exp\left\{-2\pi\lambda_{\mathrm{B},k}^s \int_{b_{k,j}(\theta_\mathrm{t})}^x t p_v(t) dt\right\}, & a = \mathrm{na} \\ \dfrac{\partial}{\partial r} F_{r_{k,\mathbf{x}_\tau}^{vj}}^{s,\mathrm{sa}}(r), & a = \mathrm{sa} \end{cases}. \tag{19}$$

Note that for the strongest association, $f^{s,\text{sa}}_{r^{vj}_{k,\mathbf{x}_\tau}}(r)$ cannot be presented due to the complicated form of (16). However, in Section IV, we show that the performance of the strongest association and that of the nearest association have similar trends. This means we can use the analysis of the nearest association to design the case of the strongest association as well.

III. OUTAGE PROBABILITY ANALYSIS

In this section, for both IS-BS and ES-BS schemes, we derive the network outage probability in the presence of GUs and AUs. The outage probability is presented for two cases: the general environment in Section III-A and the noise-limited environment in Section III-B as a special case.

A. General Environments

We assume that the available frequency resource is divided into N sub-bands, and the interfering BSs are the ones that use the same sub-band. Hence, in the IS-BS scheme, the distribution of the interfering BSs is modeled as a HPPP $\Phi_{\text{I,O}}$ with density $\lambda^{\text{IS}}_{\text{I,O}} = \lambda_{\text{B}}/N$ such as in [37]. In the ES-BS scheme, the interference from GBSs and ABSs needs to be defined differently as they use different tilt angles. The distributions of interfering GBSs and ABSs are also modeled as HPPPs, $\Phi_{\text{I,G}}$ and $\Phi_{\text{I,A}}$, with densities $\lambda^{\text{ES}}_{\text{I,G}} = \lambda^{\text{ES}}_{\text{B,G}}/N$ and $\lambda^{\text{ES}}_{\text{I,A}} = \lambda^{\text{ES}}_{\text{B,A}}/N$, respectively.

For the case that a BS communicates with the kth user, the SINR at the user can be given by

$$\gamma^s_v(r_{k,\mathbf{x}_\tau}, \theta_t) = \frac{P_t \Omega_{k,v} l_v(r_{k,\mathbf{x}_\tau}) G(r_{k,\mathbf{x}_\tau}, \theta_t)}{I^s + \sigma^2}, \quad (20)$$

where $l_v(r_{k,\mathbf{x}_\tau}) = \left(r^2_{k,\mathbf{x}} + (h_k - h_{\text{B}})^2\right)^{-\frac{\alpha_v}{2}}, v \in \{\text{L, N}\}$, is the distance-dependent path loss between the kth user and the BS at $\mathbf{x}$ for LoS and NLoS links, and σ^2 is the noise power.

In (20), $I^{\text{IS}} = I^{\text{IS}}_{\text{O}}$ and $I^{\text{ES}} = I^{\text{ES}}_{\text{G}} + I^{\text{IS}}_{\text{A}}$, where I^s_l is given by

$$I^s_l = \sum_{\mathbf{x} \in \Phi_{\text{I},l} \setminus \{\mathbf{x}_\tau\}} P_t \Omega_{k,\mathbf{x}} l_v(r_{k,\mathbf{x}}) G(r_{k,\mathbf{x}}, \theta_t). \quad (21)$$

Using the SINR in (20), when the user associates to a j-group BS with the distance $r_{k,\mathbf{x}_\tau}$ and the tilt angle θ_t under the channel environment v, the outage probability is given by

$$\mathcal{P}^v_{\text{o},j}(r_{k,\mathbf{x}_\tau}, \theta_t) = \mathbb{P}\left[\gamma^s_v(r_{k,\mathbf{x}_\tau}, \theta_t) < \gamma_t\right], \quad (22)$$

where $\gamma_t = 2^{\frac{R_o}{W}} - 1$ is the target SINR. Here, R_o is the target data rate and W is the bandwidth allocated to each user [38]. In the following theorem, we derive the network outage probability. For readability, instead of notation θ_t, when scheme s is used, we denote antenna tilt angles of the GBS and the ABS as $\theta^s_{t,\text{G}}$ and $\theta^s_{t,\text{A}}$, respectively. Note that in the IS-BS scheme, since all BSs serve both GUs and AUs, we have a single antenna tilt angle $\theta^{\text{IS}}_{t,\text{O}}$, i.e., $\theta^{\text{IS}}_{t,\text{G}} = \theta^{\text{IS}}_{t,\text{A}} = \theta^{\text{IS}}_{t,\text{O}}$.

Theorem 1: For IS-BS $(s = \text{IS})$ and ES-BS $(s = \text{ES})$ schemes, the network outage probability can be presented as a function of BS antenna tilt angles $(\theta^s_{t,\text{G}}, \theta^s_{t,\text{A}})$ as

$$\mathcal{P}^s_{\text{no}}(\theta^s_{t,\text{G}}, \theta^s_{t,\text{A}}) = \rho_{\text{G}} \underbrace{\sum_{\substack{j \in \mathcal{J}, \\ v \in \{\text{L,N}\}}} \left(\int_{b_{\text{G},j}(\theta^s_{t,\text{G}})}^{b_{\text{G},j+1}(\theta^s_{t,\text{G}})} \mathcal{A}^a_{vj} \mathcal{P}^v_{\text{o},j}(r, \theta^s_{t,\text{G}}) f^{s,a}_{r^{vj}_{\text{G}}}(r) dr\right)}_{\mathcal{P}^s_{\text{no,G}}(\theta^s_{t,\text{G}})}$$

$$+ \rho_{\text{A}} \underbrace{\sum_{\substack{j \in \mathcal{J}, \\ v \in \{\text{L,N}\}}} \left(\int_{b_{\text{A},j}(\theta^s_{t,\text{A}})}^{b_{\text{A},j+1}(\theta^s_{t,\text{A}})} \mathcal{A}^a_{vj} \mathcal{P}^v_{\text{o},j}(r, \theta^s_{t,\text{A}}) f^{s,a}_{r^{vj}_{\text{A}}}(r) dr\right)}_{\mathcal{P}^s_{\text{no,A}}(\theta^s_{t,\text{A}})}, \quad (23)$$

where $\mathcal{P}^s_{\text{no},i}(\theta^s_{t,i})$ is the network outage probability of i-type user for $s \in \{\text{IS, ES}\}$, and $\rho_i = \lambda_i/(\lambda_{\text{G}} + \lambda_{\text{A}})$ is the ratio of the density of i-type users to that of total users, $i \in \{\text{G,A}\}$, and $f^{s,a}_{r^{vj}_{k,\mathbf{x}_\tau}}(r)$ is given in (19). In (23), $\mathcal{P}^v_{\text{o},j}(r, \theta^s_{t,i})$ is given by

$$\mathcal{P}^v_{\text{o},j}(r, \theta^s_{t,i}) \quad (24)$$

$$= 1 - \sum_{n=0}^{m_v - 1} \left[\frac{(-z)^n}{n!} \frac{d^n}{dz^n} \exp(-z\sigma^2) \mathcal{L}_{I^s}(z)\right]_{z = \frac{m_v \gamma_t}{P_t l_v(r_{k,\mathbf{x}_\tau}) G_j(r, \theta^s_{t,i})}}.$$

In (24), $\mathcal{L}_{I^{\text{IS}}}(z) = \mathcal{L}_{I^{\text{IS}}_{\text{O}}}(z)$ and $\mathcal{L}_{I^{\text{ES}}}(z) = \mathcal{L}_{I^{\text{ES}}_{\text{G}}}(z)\mathcal{L}_{I^{\text{ES}}_{\text{A}}}(z)$, where $\mathcal{L}_{I^s_l}(z)$ is the Laplace transform of the interference from l-type BSs, $l \in \{\text{O,G,A}\}$, for the BS service provisioning scheme s, given in (25), shown at the top of next page. In (25), $c_{k,j}(r, \theta^s_{t,l}) = \min\left[b_{k,j+1}(\theta^s_{t,l}), \max(r, b_{k,j}(\theta^s_{t,l}))\right]$.

Proof: See Appendix A. ∎

From Theorem 1, in the general environment, we can obtain the network outage probabilities for two types of service provisioning schemes, which consider different channel fadings for LoS and NLoS environments. Here, we can see that the network outage probability is affected by the main lobe service area that the BS can serve with the strong main lobe gain, i.e., the area with distance $r^{\text{lb}}_i(\theta^s_{t,i})(= b_{k,2})$ to $r^{\text{ub}}_i(\theta^s_{t,i})(= b_{k,3})$ from a BS (see Fig. 2).

The main lobe service area is determined by the antenna tilt angle, and the effect of the antenna tilt angle on $\left|r^{\text{ub}}_i(\theta^s_{t,i}) - r^{\text{lb}}_i(\theta^s_{t,i})\right|$ is presented in the following corollary.

Corollary 1: For $\theta_{\text{th}} < \theta^s_{t,\text{G}} < \frac{\pi}{2}$ and $-\frac{\pi}{2} < \theta^s_{t,\text{A}} < -\theta_{\text{th}}$, $\left|r^{\text{ub}}_{\text{G}}(\theta^s_{t,\text{G}}) - r^{\text{lb}}_{\text{G}}(\theta^s_{t,\text{G}})\right|$ and $\left|r^{\text{ub}}_{\text{A}}(\theta^s_{t,\text{A}}) - r^{\text{lb}}_{\text{A}}(\theta^s_{t,\text{A}})\right|$ increase, as $\theta^s_{t,\text{G}}$ and $\theta^s_{t,\text{A}}$ approach θ_{th} and $-\theta_{\text{th}}$, respectively.

Proof: From (6) and (7), we obtain the first derivative of $\left|r^{\text{ub}}_{\text{G}}(\theta^s_{t,\text{G}}) - r^{\text{lb}}_{\text{G}}(\theta^s_{t,\text{G}})\right|$ with respect to $\theta^s_{t,\text{G}}$ as

$$\frac{\partial}{\partial \theta^s_{t,\text{G}}}\{r^{\text{ub}}_{\text{G}}(\theta^s_{t,\text{G}}) - r^{\text{lb}}_{\text{G}}(\theta^s_{t,\text{G}})\} = \psi(\theta^s_{t,\text{G}})(h_{\text{B}} - h_{\text{G}}) < 0, \quad (26)$$

for $\theta_{\text{th}} < \theta^s_{t,\text{G}} < \frac{\pi}{2}$, where $\psi(\theta) = \csc^2(\theta + \theta_{\text{th}}) - \csc^2(\theta - \theta_{\text{th}})$. In (26), the inequality is obtained since $\psi(\theta^s_{t,\text{G}}) < 0$ and $h_{\text{B}} - h_{\text{G}} > 0$. From (8) and (9), the first derivative of $\left|r^{\text{ub}}_{\text{A}}(\theta^s_{t,\text{A}}) - r^{\text{lb}}_{\text{A}}(\theta^s_{t,\text{A}})\right|$ with respect to $\theta^s_{t,\text{A}}$ is given by

$$\frac{\partial}{\partial \theta^s_{t,\text{A}}}\{r^{\text{ub}}_{\text{A}}(\theta^s_{t,\text{A}}) - r^{\text{lb}}_{\text{A}}(\theta^s_{t,\text{A}})\} = \psi(\theta^s_{t,\text{A}})(h_{\text{A}} - h_{\text{B}}) > 0, \quad (27)$$

for $-\frac{\pi}{2} < \theta^s_{t,\text{A}} < -\theta_{\text{th}}$. In (27), the inequality is obtained since $\psi(\theta^s_{t,\text{A}}) > 0$ and $h_{\text{A}} - h_{\text{B}} > 0$. Therefore, we can

$$\mathcal{L}_{I_l^s}(z)=\exp\left[-2\pi\lambda_{I,l}^s\sum_{j\in\mathcal{J}}\left\{\int_{c_{k,j}(r,\theta_{t,l}^s)}^{b_{k,j+1}(\theta_{t,l}^s)}tp_{\mathrm{L}}(t)\left(1-\frac{1}{\left(1+\frac{z}{m_{\mathrm{L}}}P_{\mathrm{t}}l_{\mathrm{L}}(t)G_j(t,\theta_{t,l}^s)\right)^{m_{\mathrm{L}}}}\right)dt+\int_{c_{k,j}(r,\theta_{t,l}^s)}^{b_{k,j+1}(\theta_{t,l}^s)}tp_{\mathrm{N}}(t)\left(1-\frac{1}{1+zP_{\mathrm{t}}l_{\mathrm{N}}(t)G_j(t,\theta_{t,l}^s)}\right)dt\right\}\right].$$

$$(25)$$

see that $\left|r_{\mathrm{G}}^{\mathrm{ub}}(\theta_{t,\mathrm{G}}^s)-r_{\mathrm{G}}^{\mathrm{lb}}(\theta_{t,\mathrm{G}}^s)\right|$ and $\left|r_{\mathrm{A}}^{\mathrm{ub}}(\theta_{t,\mathrm{A}}^s)-r_{\mathrm{A}}^{\mathrm{lb}}(\theta_{t,\mathrm{A}}^s)\right|$ are monotonically decreasing function and increasing function of $\theta_{t,\mathrm{G}}^s$ and $\theta_{t,\mathrm{A}}^s$, respectively. ■

Remark 1: From (6)-(9) and Corollary 1, we can see that $\left|r_i^{\mathrm{ub}}(\theta_{t,i}^s)-r_i^{\mathrm{lb}}(\theta_{t,i}^s)\right|$, $r_i^{\mathrm{lb}}(\theta_{t,i}^s)$, and $r_i^{\mathrm{ub}}(\theta_{t,i}^s)$ increases, as $\theta_{t,\mathrm{G}}^s$ or $\theta_{t,\mathrm{A}}^s$ approaches θ_{th} or $-\theta_{\mathrm{th}}$, respectively. This means the main lobe service area becomes wider as $\theta_{t,\mathrm{G}}^s$ or $\theta_{t,\mathrm{A}}^s$ approaches θ_{th} or $-\theta_{\mathrm{th}}$, respectively, as also shown in Fig. 2. However, as both $r_i^{\mathrm{lb}}(\theta_{t,i}^s)$ and $r_i^{\mathrm{ub}}(\theta_{t,i}^s)$ increases, the link distance between a BS and a user, located in the main lobe service area, becomes larger, as shown in Fig. 2. Hence, the change of the antenna tilt angle gives conflicting impacts on the network outage probability, so we need to carefully determine the antenna tilt angle to improve the network performance.

B. Special Case: Noise-Limited Environments

In this subsection, we consider the NTN for UAVs where the noise power is dominant over the interference power, i.e., the noise-limited environment.

In the noise-limited environment, for given θ_{t}, the outage probability at the kth user is defined as

$$\hat{\mathcal{P}}_{\mathrm{o},j}^v(r_{k,\mathbf{x}},\theta_{\mathrm{t}})=\mathbb{P}\left[\hat{\gamma}_v^s(r_{k,\mathbf{x}},\theta_{\mathrm{t}})\le\gamma_{\mathrm{t}}\right], \quad (28)$$

where $\hat{\gamma}_v^s(r_{k,\mathbf{x}},\theta_{\mathrm{t}})$ is obtained from (20) by substituting $I^s=0$. In the following lemma, we derive the network outage probability depending on the ratio of GUs and AUs.

Lemma 1: In the noise-limited environment, the network outage probability can be presented by a function of BS antenna tilt angles $\left(\theta_{t,\mathrm{G}}^s,\theta_{t,\mathrm{A}}^s\right)$ as

$$\hat{\mathcal{P}}_{\mathrm{no}}^s(\theta_{t,\mathrm{G}}^s,\theta_{t,\mathrm{A}}^s)=\rho_{\mathrm{G}}\sum_{\substack{j\in\mathcal{J},\\v\in\{\mathrm{L,N}\}}}\left(\int_{b_{\mathrm{G},j}(\theta_{t,\mathrm{G}}^s)}^{b_{\mathrm{G},j+1}(\theta_{t,\mathrm{G}}^s)}\mathcal{A}_{vj}^a\hat{\mathcal{P}}_{\mathrm{o},j}^v(r,\theta_{t,\mathrm{G}}^s)f_{r_{\mathrm{G}}^{vj}}^{s,a}(r)dr\right)$$
$$+\rho_{\mathrm{A}}\sum_{\substack{j\in\mathcal{J},\\v\in\{\mathrm{L,N}\}}}\left(\int_{b_{\mathrm{A},j}(\theta_{t,\mathrm{A}}^s)}^{b_{\mathrm{A},j+1}(\theta_{t,\mathrm{A}}^s)}\mathcal{A}_{vj}^a\hat{\mathcal{P}}_{\mathrm{o},j}^v(r,\theta_{t,\mathrm{A}}^s)f_{r_{\mathrm{A}}^{vj}}^{s,a}(r)dr\right), \quad (29)$$

for $s\in\{\mathrm{IS,ES}\}$, where $f_{r_{k,\mathbf{x}_\tau}^{vj}}^{s,a}(r)$ is in (19), and $\hat{\mathcal{P}}_{\mathrm{o},j}^v(r,\theta_{t,i}^s)$ is given by

$$\hat{\mathcal{P}}_{\mathrm{o},j}^v(r,\theta_{t,i}^s)=$$
$$1-\sum_{n=0}^{m_v-1}\frac{1}{n!}\left(\frac{m_v\gamma_{\mathrm{t}}\sigma^2}{P_{\mathrm{t}}l_v(r_{k,\mathbf{x}_\tau})G_j(r,\theta_{t,i}^s)}\right)^n\exp\left(-\frac{m_v\gamma_{\mathrm{t}}\sigma^2}{P_{\mathrm{t}}l_v(r_{k,\mathbf{x}_\tau})G_j(r,\theta_{t,i}^s)}\right).$$
$$(30)$$

Proof: By substituting $I^s=0$ and applying the CDF of the Gamma distribution in (39), we obtain (30). By replacing $\hat{\mathcal{P}}_{\mathrm{o},j}^v(r_{k,\mathbf{x}_\tau},\theta_{t,i}^s)$ in (42) into $\hat{\mathcal{P}}_{\mathrm{o},j}^v(r_{k,\mathbf{x}_\tau},\theta_{t,i}^s)$ and using (38), we obtain (29). ■

Let the optimal values of the BS antenna tilt angle for the IS-BS and ES-BS schemes that minimize $\hat{\mathcal{P}}_{\mathrm{no}}^{\mathrm{IS}}(\theta_{t,0})$ and $\hat{\mathcal{P}}_{\mathrm{no}}^{\mathrm{ES}}(\theta_{t,\mathrm{G}}^{\mathrm{ES}},\theta_{t,\mathrm{A}}^{\mathrm{ES}})$ be $\theta_{t,\mathrm{O}}^*$ and $\theta_{t,i}^*$, $i\in\{\mathrm{G,A}\}$, respectively. For given the optimal tilt angles, in the following corollary, we compare the network outage probabilities of the IS-BS and ES-BS schemes, i.e., $\hat{\mathcal{P}}_{\mathrm{no}}^{\mathrm{IS}}(\theta_{t,\mathrm{O}}^*)$ and $\hat{\mathcal{P}}_{\mathrm{no}}^{\mathrm{ES}}(\theta_{t,\mathrm{G}}^*,\theta_{t,\mathrm{A}}^*)$.

Corollary 2: When the density of BSs approaches to infinity (i.e., $\lambda_{\mathrm{B}}\to\infty$) and the optimal tilt angles are used for each scheme, the network outage probability of the ES-BS scheme is smaller than or equal to that of the IS-BS scheme, i.e.,

$$\hat{\mathcal{P}}_{\mathrm{no}}^{\mathrm{IS}}(\theta_{t,\mathrm{O}}^*)\ge\hat{\mathcal{P}}_{\mathrm{no}}^{\mathrm{ES}}(\theta_{t,\mathrm{G}}^*,\theta_{t,\mathrm{A}}^*). \quad (31)$$

Proof: When λ_{B} approaches to infinity, $\lambda_{\mathrm{B,G}}^s$ and $\lambda_{\mathrm{B,A}}^s$ also approach to infinity, respectively. Hence, in (19), regardless of the service provisioning scheme, the PDFs of the horizontal distance between the kth user and the serving BS become similar, i.e., $f_{r_{k,\mathbf{x}_\tau}^{vj}}(r)\approx f_{r_{k,\mathbf{x}_\tau}^{vj}}^{\mathrm{IS},a}(r)\approx f_{r_{k,\mathbf{x}_\tau}^{vj}}^{\mathrm{ES},a}(r)$. Substituting $f_{r_{k,\mathbf{x}_\tau}^{vj}}(r)$ and $\hat{\mathcal{P}}_{\mathrm{o},j}^v(r,\theta_{t,i}^s)$ into (42), and using the optimal antenna tilt angles, the network outage probabilities of i-type users for the IS-BS scheme and the ES-BS scheme, $\hat{\mathcal{P}}_{\mathrm{no},i}^{\mathrm{IS}}(\theta_{t,\mathrm{O}}^*)$ and $\hat{\mathcal{P}}_{\mathrm{no},i}^{\mathrm{ES}}(\theta_{t,i}^*)$, can be represented as

$$\hat{\mathcal{P}}_{\mathrm{no},i}^{\mathrm{IS}}(\theta_{t,\mathrm{O}}^*)=\sum_{\substack{j\in\mathcal{J},\\v\in\{\mathrm{L,N}\}}}\left(\int_{b_{k,j}(\theta_{t,\mathrm{O}}^*)}^{b_{k,j+1}(\theta_{t,\mathrm{O}}^*)}\mathcal{A}_{vj}^a\hat{\mathcal{P}}_{\mathrm{o},j}^v(r,\theta_{t,\mathrm{O}}^*)f_{r_{k,\mathbf{x}_\tau}^{vj}}(r)dr\right),$$
$$\hat{\mathcal{P}}_{\mathrm{no},i}^{\mathrm{ES}}(\theta_{t,i}^*)=\sum_{\substack{j\in\mathcal{J},\\v\in\{\mathrm{L,N}\}}}\left(\int_{b_{k,j}(\theta_{t,i}^*)}^{b_{k,j+1}(\theta_{t,i}^*)}\mathcal{A}_{vj}^a\hat{\mathcal{P}}_{\mathrm{o},j}^v(r,\theta_{t,i}^*)f_{r_{k,\mathbf{x}_\tau}^{vj}}(r)dr\right).$$
$$(32)$$

In (32), we can always obtain $\hat{\mathcal{P}}_{\mathrm{no},i}^{\mathrm{IS}}(\theta_{t,\mathrm{O}}^*)\ge\hat{\mathcal{P}}_{\mathrm{no},i}^{\mathrm{ES}}(\theta_{t,i}^*)$, $\forall i\in\{\mathrm{G,A}\}$ because $\theta_{t,\mathrm{G}}^*$ and $\theta_{t,\mathrm{A}}^*$ in the ES-BS scheme are optimized ones for GUs and AUs, respectively, while in the IS-BS scheme, $\theta_{t,\mathrm{O}}^*$ is optimized one for both type users to minimize the total network outage probability. Therefore, from (38), we can conclude as (31). ■

From Corollary 2, we can see that when the density of BSs is sufficiently large, the ES-BS scheme outperforms the IS-BS scheme in terms of the network outage probability. Therefore, when the number of BSs is large enough, it is beneficial to exclusively serve GUs and AUs by independently optimizing the BS antenna tilt angles. This is also verified in Section IV, through the simulation results.

In noise-limited environments, to obtain the insight of network parameters on the network outage probability, we simplify the antenna gain model in (10) as

$$\tilde{G}(r_{k,\mathbf{x}},\theta_{\mathrm{t}})=\begin{cases}\tilde{G}_1,&b_{k,1}(\theta_{\mathrm{t}})<r_{k,\mathbf{x}}<b_{k,2}(\theta_{\mathrm{t}})\\\tilde{G}_2,&b_{k,2}(\theta_{\mathrm{t}})\le r_{k,\mathbf{x}}\le b_{k,3}(\theta_{\mathrm{t}})\\\tilde{G}_3,&b_{k,3}(\theta_{\mathrm{t}})<r_{k,\mathbf{x}}<b_{k,4}(\theta_{\mathrm{t}})\end{cases}, \quad (33)$$

TABLE II
ENVIRONMENT PARAMETERS

Parameters	Values	Parameters	Values
α_{L}	2.5	α_{N}	3.5
P_{t} [W]	3.5	σ^2 [W]	10^{-9}
μ	0.5	ν	3×10^{-4}
ξ	40	γ_{t}	1
m	3	h_{B} [m]	30
h_{G} [m]	0	h_{A} [m]	20
λ_{B} [BSs/m^2]	10^{-5}	ρ_{G}	0.5

PSfrag replacements

Fig. 3. Network outage probability of the AUs as a function of h_{A} for different AU height distributions and the BS density.

where $\tilde{G}_1 = \tilde{G}_3$ is the constant antenna side lobe gain and $\tilde{G}_2$ is the constant antenna main lobe gain. We then obtain the network outage probability as in the following corollary.

Corollary 3: When $p_{\mathrm{N}}(r_{k,\mathbf{x}}) = 1$ and $\alpha_{\mathrm{N}} = 4$, the network outage probability with the simplified antenna gain model in (33) is given by

$$\tilde{\mathcal{P}}_{\mathrm{no}}^s\left(\theta_{\mathrm{t,G}}^s, \theta_{\mathrm{t,A}}^s\right) = 1 - \sum_{\substack{j \in \mathcal{J}, \\ i \in \{\mathrm{G,A}\}}} \rho_i \left\{ g_j\left(b_{i,j+1}(\theta_{\mathrm{t},i}^s)\right) - g_j\left(b_{i,j}(\theta_{\mathrm{t},i}^s)\right) \right\}$$
$$\times \frac{\sqrt{\tilde{G}_j} \pi^{\frac{3}{2}} \lambda_{\mathrm{B},i}^s \exp\left(\frac{4\omega \tilde{h}_i^2 + \pi \tilde{G}_j \lambda_{\mathrm{B},i}^s}{4\omega}\right)}{2\sqrt{\omega}}, \quad (34)$$

where $\tilde{h}_i = |h_{\mathrm{B}} - h_i|$, $\omega = \frac{\gamma_{\mathrm{t}} \sigma^2}{P_{\mathrm{t}}}$, and $g_j(b)$ is given by

$$g_j(b) = \mathrm{erf}\left(\frac{\tilde{G}_j \lambda_{\mathrm{B},i}^s \pi + 2\omega\left(\sqrt{(b^2 + \tilde{h}_i^2)^2}\right)}{2\sqrt{\omega \tilde{G}_j}}\right). \quad (35)$$

Proof: From (30), by substituting $p_{\mathrm{N}}(r_{k,\mathbf{x}_\tau}) = 1$, $\alpha_{\mathrm{N}} = 4$, and $G(r_{k,\mathbf{x}_\tau}, \theta_{\mathrm{t},i}^s) = \tilde{G}(r_{k,\mathbf{x}_\tau}, \theta_{\mathrm{t},i}^s)$, $\mathcal{P}_{\mathrm{o},j}(r_{k,\mathbf{x}_\tau}, \theta_{\mathrm{t},i}^s)$ is represented by

$$\tilde{\mathcal{P}}_{\mathrm{o},j}(r_{k,\mathbf{x}_\tau}, \theta_{\mathrm{t},i}^s) = 1 - \exp\left(-\frac{\gamma_{\mathrm{t}} \sigma^2 \left(\sqrt{r_{k,\mathbf{x}_\tau}^2 + \tilde{h}_i^2}\right)^4}{P_{\mathrm{t}} \tilde{G}_j}\right). \quad (36)$$

Similar to (42), after averaging $\tilde{\mathcal{P}}_{\mathrm{o},j}(r_{k,\mathbf{x}_\tau}, \theta_{\mathrm{t},i}^s)$ over $r_{k,\mathbf{x}_\tau}$, we obtain the network outage probability of i-type user, $\tilde{\mathcal{P}}_{\mathrm{no},i}(r_{k,\mathbf{x}_\tau}, \theta_{\mathrm{t},i}^s)$ as

$$\tilde{\mathcal{P}}_{\mathrm{no},i}^s(\theta_{\mathrm{t},i}^s) = 1 - \sum_{j \in \mathcal{J}} \int_{b_{i,j}(\theta_{\mathrm{t},i}^s)}^{b_{i,j+1}(\theta_{\mathrm{t},i}^s)} \exp\left(-\frac{\omega\left(\sqrt{r^2 + \tilde{h}_i^2}\right)^4}{\tilde{G}_j}\right) \tilde{f}_{r_k}^s(r) dr, \quad (37)$$

where $\tilde{f}_{r_k}^s(r) = 2\pi \lambda_{\mathrm{B},i}^s r \exp\left(-\pi \lambda_{\mathrm{B},i}^s r^2\right)$ and $\tilde{f}_{r_k}^s(r) = \tilde{f}_{r_i}^s(r)$ for $k \in \mathcal{U}_i$. From (37), by using result in [39, eq. (3.322)] and (38), we obtain (34). ∎

In Corollary 3, we obtain the network outage probability in the noise-limited environment as a closed form.
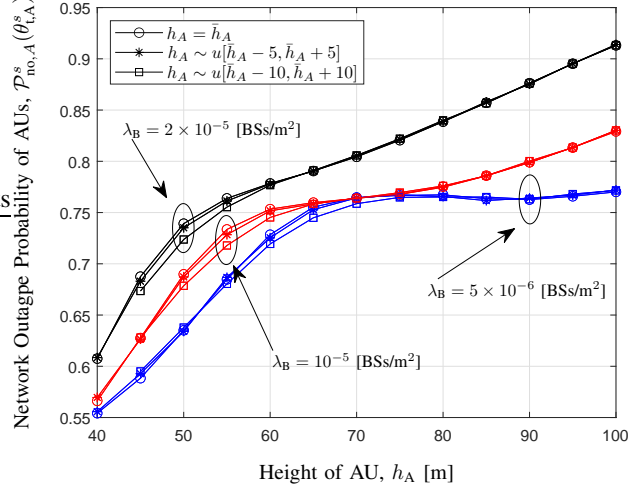
IV. NUMERICAL RESULTS

In this section, we evaluate the effect of the BS antenna tilt angle, the BS density, the interfering BS density, and the network parameters on the network outage probability. We first show the network outage probability on each of the IS-BS and ES-BS schemes. We then compare the performance of the service provisioning schemes. In the numerical results, for the convenience of explanation, we denote the total interfering density as λ_{I} regardless of the scheme, i.e., $\lambda_{\mathrm{I}} = \lambda_{\mathrm{I,O}}^{\mathrm{IS}} = \lambda_{\mathrm{I,G}}^{\mathrm{ES}} + \lambda_{\mathrm{I,A}}^{\mathrm{ES}}$. Unless otherwise specified, we use the simulation parameters given in Table II based on the 3GPP specification and consider the dense urban environment parameters μ, ν and ξ [40], [41].

Figure 3 presents the network outage probability of AUs for the cases of the fixed height $\bar{h}_A$ and the uniform distribution height (i.e., $h_{\mathrm{A}} \sim u[\bar{h}_A - \delta, \bar{h}_A + \delta]$). As shown in this figure, the trends of network outage probability with the random height are similar to that with the fixed height only. Therefore, from this result, we show that only the performance of the fixed height case in the following figures. Even though there is a gap between the performance of the random height and that of the fixed height, the optimal height that minimizes network outage probability is almost the same.

A. Network Outage Probability of Ground and Air Users

In this subsection, we analyze the impact of the BS antenna tilt angle on the network outage probabilities of GUs and AUs.

Figure 4 presents the network outage probability of i-type user, $\mathcal{P}_{\mathrm{no},i}^s(\theta_{\mathrm{t},i}^s)$, as a function of the BS antenna tilt angle, $\theta_{\mathrm{t},i}^s$, for different channel environments and BS association rules. Here, we use $\lambda_{\mathrm{I}} = 0.5\lambda_{\mathrm{B}}$. From Fig. 4, for GUs ($i = \mathrm{G}$) in the general environment, we can see that as $\theta_{\mathrm{t},i}^s$ increases, $\mathcal{P}_{\mathrm{no},i}^s(\theta_{\mathrm{t},i}^s)$ first increases up to a certain value of $\theta_{\mathrm{t},i}^s$, and then decreases. This is because as $\theta_{\mathrm{t},i}^s$ increases, the number of interfering BSs that form the antenna main lobe gain to the GU increases i.e., the GU receives larger interference. However, for relatively large $\theta_{\mathrm{t},i}^s$ (e.g., $0° < \theta_{\mathrm{t},i}^s < 15°$), the desired BS can transmit the signal with the antenna main lobe gain to the GU
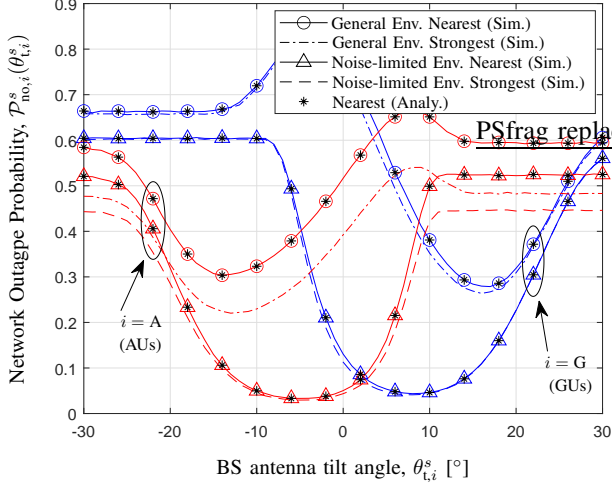
Fig. 4. Network outage probability of i-type user as a function of $\theta_{t,i}^s$ for different environments and BS association rules.

Fig. 5. Network outage probability of i-type user $\mathcal{P}_{no,i}^s(\theta_{t,i}^s)$ as a function of $\theta_{t,i}^s$ for different values of λ_I. The optimal BS antenna tilt angles, $\theta_{t,i}^*$, that minimize $\mathcal{P}_{no,i}^s(\theta_{t,i}^s)$ are marked by dashed circles.

mostly, while the number of interfering BSs with the antenna main lobe gain to the GU decreases. Therefore, $\mathcal{P}_{no,i}^s(\theta_{t,i}^s)$ decreases with $\theta_{t,i}^s$. Furthermore, when $\theta_{t,i}^s$ is much large (e.g., $\theta_{t,i}^s > 20°$), as $\theta_{t,i}^s$ increases, the desired BS transmits the signal with the antenna side lobe gain to the GU with high probability. In this case, the performance loss of the main link is dominant, so $\mathcal{P}_{no,i}^s(\theta_{t,i}^s)$ increases again. For AUs ($i = A$), the trend becomes opposite, but the reason is the same as the case of GUs.

In the noise-limited environment, the main link channel's quality, which is affected by the antenna gain, mainly determines the network performance. Hence, we observe that as $\theta_{t,i}^s$ increases, $\mathcal{P}_{no,i}^s(\theta_{t,i}^s)$ first decreases and then increases. This is because as $\theta_{t,i}^s$ increases, the main lobe of serving BS is first closer to the user, and then get further away.

We can also see that our analysis is well matched with the simulation results. Furthermore, the network outage probability with the strongest association rule has a similar trend to that with the nearest association rule. The network outage probability of the nearest association is always higher than that of the strongest association. Hence, in the following figures, we present the numerical results of the nearest association only.

Figure 5 presents the network outage probability of i-type user, $\mathcal{P}_{no,i}^s(\theta_{t,i}^s)$, as a function of the BS antenna tilt angle, $\theta_{t,i}^s$, for different values of the interfering BS density, λ_I. From Fig. 5, we can see that as λ_I increases, the absolute value of the optimal tilt angle for i-type user, $\theta_{t,i}^*$, which is marked by the dashed circle in the figure, increases. This is to ensure that the number of interfering BSs with the antenna main lobe gain to the GU or AU decreases, as the number of interfering BSs increases. Moreover, when λ_I is much small (e.g., $\lambda_I \leq 0.01\lambda_B$), we can also observe that the network outage probability in the general environment approaches that in the noise-limited environment.

B. Results of IS-BS Scheme

In this subsection, we analyze the impact of the BS antenna tilt angle on the network outage probability with the IS-BS
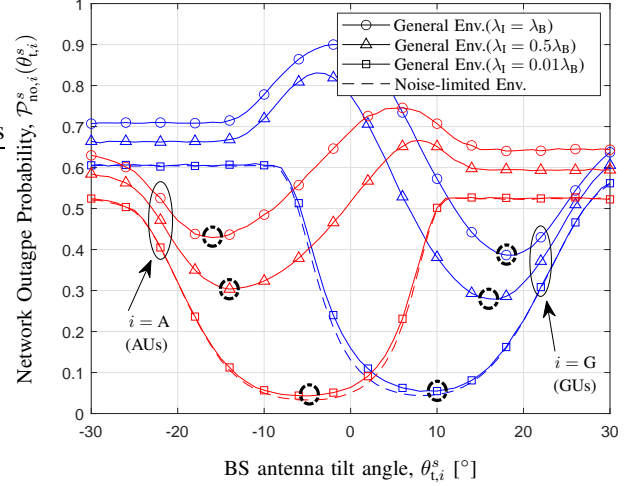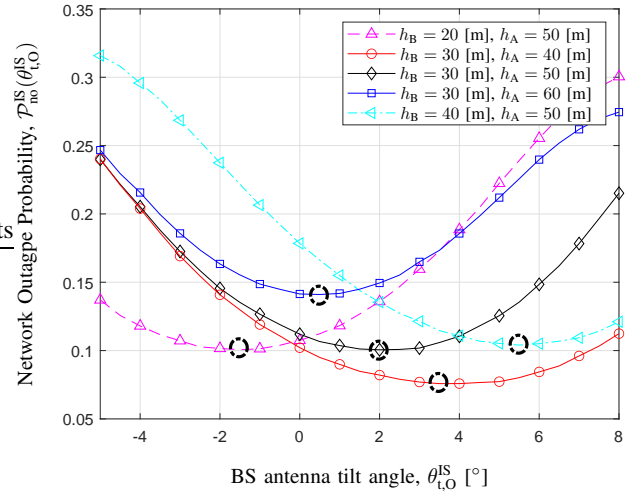

Fig. 6. Network outage probability $\mathcal{P}_{no}^{IS}(\theta_{t,O}^{IS})$ as a function of $\theta_{t,O}^{IS}$ for different values of h_B and h_A with $\lambda_I = 0.01\lambda_B$. The optimal BS antenna tilt angles, $\theta_{t,O}^*$, that minimize $\mathcal{P}_{no}^{IS}(\theta_{t,O}^{IS})$ are marked by dashed circles.

scheme.

Figure 6 presents the network outage probability of the IS-BS scheme, $\mathcal{P}_{no}^{IS}(\theta_{t,O}^{IS})$, as a function of the BS antenna tilt angle, $\theta_{t,O}^{IS}$, for different values of the BS height, h_B, and the AU height, h_A. Here, we use $\lambda_I = 0.01\lambda_B$ (i.e., similar to the noise-limited environment). From Fig. 6, we can see that for the fixed height of AUs (e.g., $h_A = 50$ m), as the height of the BS increases (e.g., $h_B = 20 \sim 40$ m), the optimal value of the BS antenna tilt angle, $\theta_{t,O}^*$, which is marked by the dashed circle in the figure, increases. For AUs, as h_B increases, the LoS probability between the BS and the AU increases and the distance-dependent path loss decreases. Hence, the performance of AUs can be significantly improved by the high LoS probability and low path loss. On the other hand, for GUs, as h_B increases, the LoS probability between the BS and the GU increases, while the distance-dependent path loss increases due to the increased distance from the BS to the GU and it is harmful to the GU. Consequently, as h_B increases, since GUs
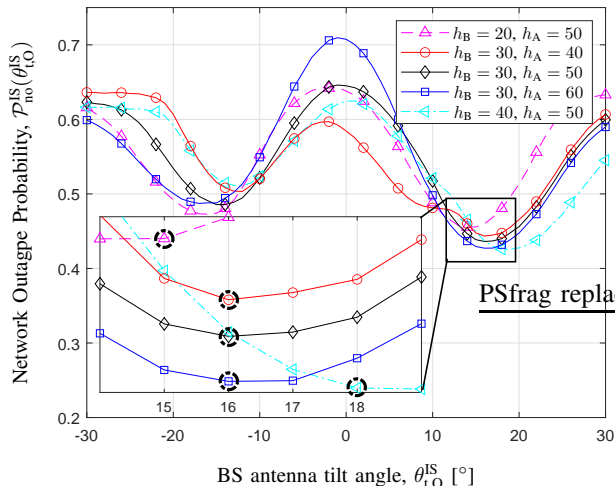
Fig. 7. Network outage probability $\mathcal{P}_{\mathrm{no}}^{\mathrm{IS}}(\theta_{\mathrm{t,O}}^{\mathrm{IS}})$ as a function of $\theta_{\mathrm{t,O}}^{\mathrm{IS}}$ for different values of h_{B} and h_{A} with $\lambda_{\mathrm{I}} = 0.5\lambda_{\mathrm{B}}$. The optimal BS antenna tilt angles, $\theta_{\mathrm{t,O}}^{*}$, that minimize $\mathcal{P}_{\mathrm{no}}^{\mathrm{IS}}(\theta_{\mathrm{t,O}}^{\mathrm{IS}})$ are marked by dashed circles.

Fig. 8. Optimal BS antenna tilt angle, $\theta_{\mathrm{t,O}}^{*}$, according to ρ_{G} for different values of λ_{B} in the IS-BS scheme.

experience relatively worse channel condition compared to AUs, the optimal values of the BS antenna tilt angle increases to downward to compensate the performance loss of GUs.

In this figure, we can also observe that for the fixed height of BSs (e.g. $h_{\mathrm{B}} = 30$ m), as the height of the AU increases (e.g. $h_{\mathrm{A}} = 40 \sim 60$ m), the minimum network outage probability, which is a value of the dashed circle in the y-axis, increases and the optimal value of the BS antenna tilt angle, which is a value of the dashed circle in the x-axis, decreases. As h_{A} increases, the LoS probability between the BS and AU and the distance-dependent path loss increases. However, since the effect of the path-loss increasing is greater, the outage probability of AU increases. On the other hand, the performance of GUs is not affected by h_{A}. Therefore, the optimal antenna tilt angle decreases to be compensated for the performance loss of AUs.

Figure 7 presents the network outage probability of the IS-BS scheme, $\mathcal{P}_{\mathrm{no}}^{\mathrm{IS}}(\theta_{\mathrm{t,O}}^{\mathrm{IS}})$, as a function of the BS antenna tilt angle, $\theta_{\mathrm{t,O}}^{\mathrm{IS}}$, for different values of the BS height, h_{B}, and the AU height, h_{A}, similar to Fig. 6. Here, we use $\lambda_{\mathrm{I}} = 0.5\lambda_{\mathrm{B}}$. From Fig. 7, we can see that the optimal values of the BS antenna tilt angle, $\theta_{\mathrm{t,O}}^{*}$, exist in the considerably down tilted regions compared to Fig. 6. As shown in Fig. 5, the difference of the optimal antenna tilt angles for GUs and AUs increases as λ_{I} increases. Consequently, in terms of the network performance of the IS-BS scheme, it is worth optimizing the antenna tilt angle toward a certain type of users, i.e., GUs and AUs. Specifically, for a given configuration, AUs are more affected by interference due to high LoS probability than GUs, hence BSs transmit the signal to AUs with the side lobe to reduce interfering signal power. On the other hand, to increase the main link power, BSs transmit the signal to GUs with the main lobe. Therefore, to minimize network outage probability, the BS antenna needs to be tilted downwards.

We can also see that for the fixed height of AUs (e.g., $h_{\mathrm{A}} = 50$ m), as the height of the BS increases (e.g., $h_{\mathrm{B}} = 20 \sim 40$ m), the optimal value of the BS antenna tilt angle increases.
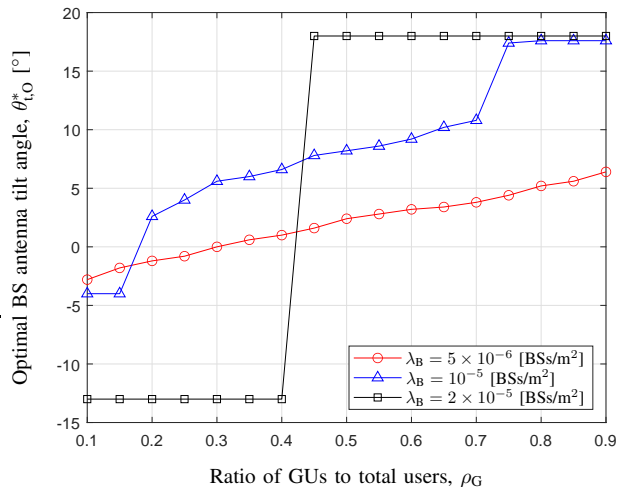
This is to reduce the number of interfering BSs which has the antenna main lobe gain to GUs and ensure that most serving BS transmits the signal with the antenna main lobe gain to GUs. On the contrary, for the fixed height of BSs (e.g., $h_{\mathrm{B}} = 30$ m), there is no change in the value of optimal tilt angle according to h_{A}, because AUs are served by the side lobe.

Figure 8 presents the optimal value of the BS antenna tilt angle, $\theta_{\mathrm{t,O}}^{*}$, according to the ratio of GUs to total users, ρ_{G}, for different values of the total BS density, λ_{B}, with the IS-BS scheme. Here, we use $\lambda_{\mathrm{I}} = 0.1\lambda_{\mathrm{B}}$. From Fig. 8, we can see that as ρ_{G} increases, the optimal value of the BS antenna tilt angle, $\theta_{\mathrm{t,O}}^{*}$, also increases. Since the interference is not significant in this environment, the main link channel's quality mainly determines the network performance dominantly. Hence, as the portion of GUs increases, the BS needs to tilt its antenna downward. For large λ_{B} (e.g., $\lambda_{\mathrm{B}} \geq 2 \times 10^{-5}$), we can also observe that the value of the optimal antenna tilt angle is either downwards (e.g., $\theta_{\mathrm{t,O}}^{*} = 18°$) or upwards (e.g., $\theta_{\mathrm{t,O}}^{*} = -13°$). Because of the significant difference of the optimal antenna tilt angles for GUs and AUs, it is worth optimizing the antenna tilt angle toward a certain type of users, as also explained in Fig. 7.

C. Results of ES-BS Scheme

In this subsection, we analyze the impact of the BS antenna tilt angle on the network outage probability with the ES-BS scheme. Note that, in the ES-BS scheme, since the GUs and AUs are exclusively served by the BSs, the antenna tilt angles for GUs, $\theta_{\mathrm{t,G}}^{\mathrm{ES}}$, and AUs, $\theta_{\mathrm{t,A}}^{\mathrm{ES}}$, are independently designed to minimize the network outage probability. Furthermore, in the ES-BS scheme, the ratio of GBSs affects the optimal BS tilt angles and hence, we optimize the BS tilt angles in accordance with the ratio of GBSs to total BSs, $\rho_{\mathrm{B,G}}$.

Figure 9 shows the optimal ratio of GBSs to total BSs, $\rho_{\mathrm{B,G}}^{*}$, that minimizes the network outage probability, according to the GU ratio to total users, ρ_{G}. We consider different values of the total BS density, λ_{B}, and we use $\lambda_{\mathrm{I}} = 0.1\lambda_{\mathrm{B}}$. Here, for given ρ_{G}, λ_{B}, and $\rho_{\mathrm{B,G}}$, the BS antenna tilt angles $\theta_{\mathrm{t,G}}^{\mathrm{ES}}$ and $\theta_{\mathrm{t,A}}^{\mathrm{ES}}$ are
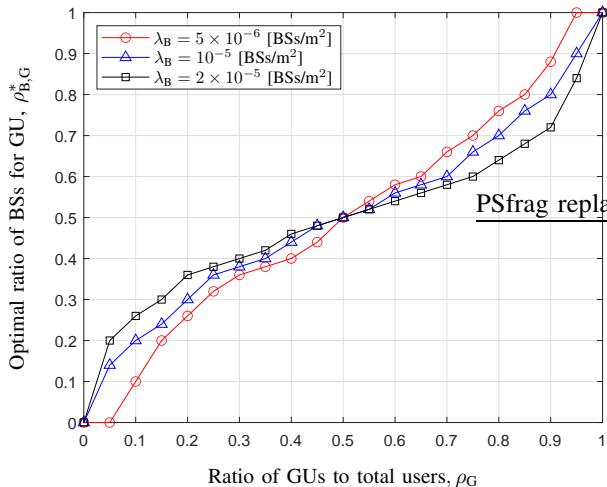
Fig. 9. Optimal ratio of BSs for GUs to total BS $\rho_{B,G}$ according to ρ_G for different values of λ_B in the ES-BS scheme.
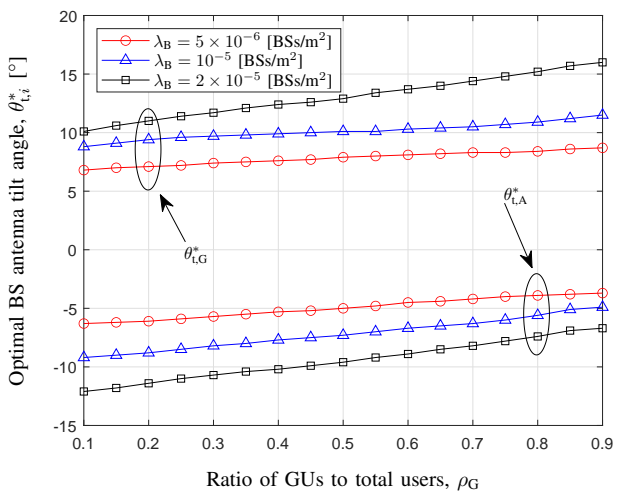

Fig. 10. Optimal BS antenna tilt angle ($\theta_{t,G}^*$, and $\theta_{t,A}^*$) according to ρ_G for different values of λ_B in the ES-BS scheme.

also optimized to minimize the network outage probability. In Fig. 9, as ρ_G increases, $\rho_{B,G}^*$ also increases because it is beneficial to have more GBSs when the portion of GUs is large. We can also see that for large ρ_G (e.g., $\rho_G > 0.5$), $\rho_{B,G}^*$ becomes smaller as λ_B increases. This is because as there is more the number of BSs, we can have a sufficient number of GBSs, so we can assign a larger portion of BSs as the ABSs. On the contrary, when ρ_G is small (e.g., $\rho_G < 0.5$), $\rho_{B,G}^*$ becomes larger as λ_B increases for a similar reason.

Figure 10 presents the optimal value of the BS antenna tilt angles, $\theta_{t,G}^*$ and $\theta_{t,A}^*$, according to the ratio of GUs to total users, ρ_G, for different values of the total BS density, λ_B, with ES-BS scheme. Here, we use $\lambda_I = 0.1\lambda_B$. From Fig. 10, we can see that as ρ_G increases, the absolute values of $\theta_{t,G}^*$ and $\theta_{t,A}^*$ also increase. In the ES-BS scheme, as ρ_G increases $\rho_{B,G}^*$ also increases, as shown in Fig. 9. Therefore, as the number of BSs increases, to reduce the number of interfering BSs giving the large interference with the antenna main lobe gain, the antenna is tilted more downwards or upwards. For the same
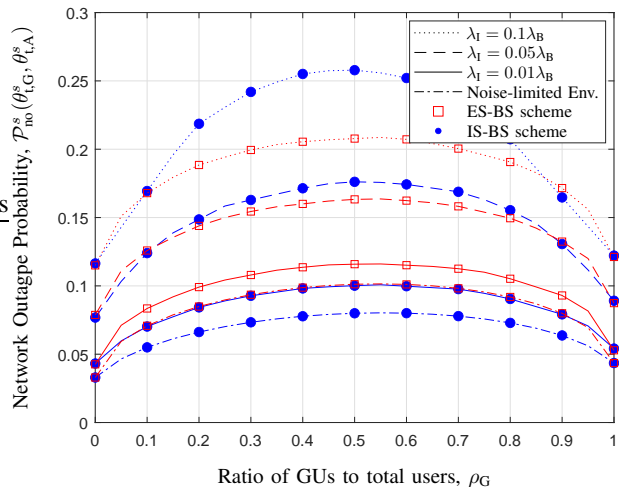

Fig. 11. Network outage probability according to ρ_G with different values of λ_I of IS-BS scheme and ES-BS scheme.

reason, we can observe that for given ρ_G, as λ_B increases, the absolute values of $\theta_{t,G}^*$ and $\theta_{t,A}^*$ also increase.

D. Comparison between IS-BS Scheme and ES-BS Scheme

In this subsection, we compare the performance of the BS service provisioning schemes in terms of the network outage probability according to the ratio of GUs to total users, ρ_G. As a baseline scheme, we also plot the service provisioning scheme that the BS antenna is tilted toward GUs without considering AUs as in conventional cellular networks. In this baseline scheme, the BS optimizes the antenna tilt angle to minimize the outage probability of GUs. For the comparison of the IS-BS scheme and the ES-BS scheme, the antenna tilt angle of the IS-BS scheme ($\theta_{t,O}^{IS}$), that of the ES-BS scheme ($\theta_{t,G}^{ES}, \theta_{t,A}^{ES}$), and the ratio of GBSs ($\rho_{B,G}$) are optimized, respectively.

Figure 11 presents the network outage probability, $\mathcal{P}_{no}^s(\theta_{t,G}^s, \theta_{t,A}^s)$, as a function of the ratio of GUs, ρ_G, for different values of λ_I and service provisioning schemes. From Fig. 11, we can see that when λ_I is large (e.g., $\lambda_I \geq 0.05\lambda_B$), the ES-BS scheme outperforms the IS-BS scheme. This is because, for the ES-BS scheme, most of the interference from other types of BSs mostly transmits the signal to user with antenna side lobe gain. On the other hand, for small λ_I (e.g., $\lambda_I \leq 0.01\lambda_B$) and the noise-limited environment, the IS-BS scheme performs better than the ES-BS scheme. This is because the effect of the interference is relatively small, so more serving BSs candidates (i.e., $\lambda_{B,i}^{IS} > \lambda_{B,i}^{ES}$) improve the performance of the main link.

Figure 12 presents the network outage probability in noise-limited environments, $\hat{\mathcal{P}}_{no}^s(\theta_{t,G}^s, \theta_{t,A}^s)$, as a function of the ratio of GUs ρ_G for different values of the total BS density λ_B and different service provisioning schemes. From Fig. 12, we can see that when the total BS density is small (e.g., $\lambda_B \leq 10^{-5}$), the IS-BS scheme outperforms the ES-BS scheme. On the contrary, for the large total BS density (e.g., $\lambda_B \geq 2 \times 10^{-5}$), the ES-BS scheme provides better performance than the IS-BS scheme in terms of the network outage probability. From these observations, we can find that when there exist
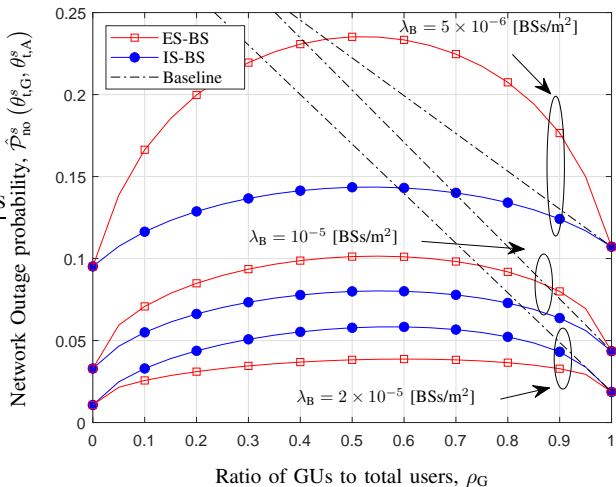
Fig. 12. Network outage probability according to the GU ratio with different total BS density λ_B of IS-BS scheme, ES-BS scheme, and baseline scheme in the noise-limited environment.
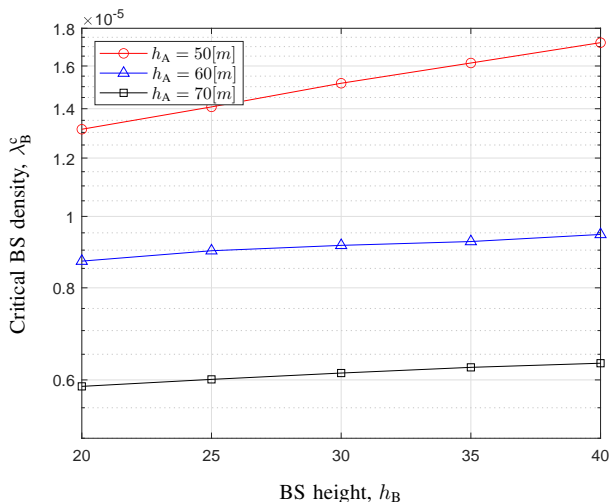

Fig. 13. Critical BS density λ_B^c according to h_B with different values h_A

enough BSs in the network, it is beneficial to exclusively serve each type of user by independently optimizing the BS antenna tilt angle for each type of user (ES-BS scheme). On the other hand, when the number of BSs is relatively small, the efficient service provisioning scheme is that all BSs serve both GUs and AUs by optimizing the BS antenna tilt angle to maximize the network performance (IS-BS scheme). We can also see that regardless of λ_B and ρ_G, the service provisioning schemes outperform the baseline scheme because the schemes design the BS antenna tilt angle by considering AUs as well as GUs.

In Corollary 2 and Fig. 12, we show that when λ_I is very small (i.e., noise-limited environments), the ES-BS scheme outperforms the IS-BS scheme for large λ_B, but the IS-BS scheme provides better performance than the ES-BS scheme for small λ_B. Therefore, there exist the value of λ_B that makes the performance of two service provisioning schemes to be equal such as $\mathcal{P}_{no}^{IS}(\theta_{t,O}^{IS}) = \mathcal{P}_{no}^{ES}(\theta_{t,G}^{ES}, \theta_{t,A}^{ES})$, and we define this value of λ_B as the *critical density of BSs*, λ_B^c. That means in the region of $\lambda_B < \lambda_B^c$, the IS-BS scheme is superior to the

ES-BS scheme in terms of the network outage probability and vice versa.

Figure 13 presents the critical density of the BS, λ_B^c, as a function of the BS height, h_B, for the different values of the AU height, h_A. In this figure, we can see that as the distance between the BS and the AU becomes closer, (i.e., h_B increases for given h_A or the h_A decreases for given h_B), λ_B^c increases. In this case, since the performance of the AUs is good enough due to the relatively short distance, the BS in the IS-BS scheme mainly tilt the antenna for GUs to enhance the network performance. Therefore, the IS-BS scheme can provide better performance than the ES-BS scheme. In contrast, for the case that the BS is far from the AUs, the BS in the IS-BS scheme has to properly tilt the antenna by considering the performance of both GU and AU. Therefore, in this case, the ES-BS scheme can be more efficient as it can be independently optimized the antenna tilt angles for GUs and AUs, respectively.

V. CONCLUSION

This paper explores an appropriate BS service provisioning scheme to serve both GUs and AUs by considering tilt angle-based antenna gain. We first derive the network outage probability for two types of provisioning schemes, i.e., IS-BS scheme and ES-BS scheme (in Theorem 1). We then explore the conflict impact of the antenna tilt angle on the network outage probability, i.e., as the absolute value of the tilt angle decreases, the main lobe service area becomes wider, but the main link distance increases (in Corollary 1 and Remark 1). From this relation, we numerically show that there exists the optimal BS antenna tilt angle that minimizes the network outage probability. Moreover, we show the impact of the ratio of GUs, the BS height, the UAV height, and densities of the total BSs and the interfering BSs on the optimal tilt angle as well as network outage probabilities for two service provisioning schemes. Finally, for given network parameters, we present which service provisioning scheme is more appropriate. Specifically, in Corollary 3, we show that the ES-BS scheme is better than the IS-BS scheme when BSs are densely deployed. In contrast, the IS-BS scheme performs better than the ES-BS scheme for low BS density or interfering BS density. The outcomes of this work can be useful for the optimal antenna tilt angle design and the BS provisioning service scheme determination in the networks, where both GUs and AUs exist.

APPENDIX

A. Proof of Theorem 1

For the given ratio of GUs and AUs, ρ_G and ρ_A, the network outage probability can be presented by

$$\mathcal{P}_{no}^s(\theta_{t,G}^s, \theta_{t,A}^s) \overset{(a)}{=} \rho_G \mathcal{P}_{no,G}^s(\theta_{t,G}^s) + \rho_A \mathcal{P}_{no,A}^s(\theta_{t,A}^s), \ s \in \{\text{IS}, \text{ES}\}, \ (38)$$

where $\mathcal{P}_{\mathrm{no},i}^s(\theta_{\mathrm{t},i}^s)$ is the network outage probability of i-type users and (a) is from the law of total probability. From (20) and (22), $\mathcal{P}_{\mathrm{o},j}^v(r_{k,\mathbf{x}_\tau}^{vj}, \theta_{\mathrm{t},i}^s)$ can be presented by

$$\mathcal{P}_{\mathrm{o},j}^v(r_{k,\mathbf{x}_\tau}^{vj}, \theta_{\mathrm{t},i}^s) = \mathbb{P}\left[\Omega_{k,\mathbf{x}_\tau} < \frac{\gamma_{\mathrm{t}}(I^s + \sigma^2)}{P_{\mathrm{t}} l_v\left(r_{k,\mathbf{x}_\tau}^{vj}\right) G_j\left(r_{k,\mathbf{x}_\tau}^{vj}, \theta_{\mathrm{t},i}^s\right)}\right]$$

$$\overset{(a)}{=} 1 - \mathbb{E}_{I^s}\left[\frac{\gamma\left(m_v, \frac{m_v \gamma_{\mathrm{t}}(I^s + \sigma^2)}{P_{\mathrm{t}} l_v(r_{k,\mathbf{x}_\tau}^{vj}) G_j(r_{k,\mathbf{x}_\tau}^{vj}, \theta_{\mathrm{t},i}^s)}\right)}{\Gamma(m_v)}\right]$$

$$\overset{(b)}{=} 1 - \mathbb{E}_{I^s}\left[\sum_{n=0}^{m_v-1} \frac{1}{n!}\left(\frac{m_v \gamma_{\mathrm{t}}(I^s + \sigma^2)}{P_{\mathrm{t}} l_v\left(r_{k,\mathbf{x}_\tau}^{vj}\right) G_j\left(r_{k,\mathbf{x}_\tau}^{vj}, \theta_{\mathrm{t},i}^s\right)}\right)^n\right.$$

$$\left.\times \exp\left(-\frac{m_v \gamma_{\mathrm{t}}(I^s + \sigma^2)}{P_{\mathrm{t}} l_v\left(r_{k,\mathbf{x}_\tau}^{vj}\right) G_j\left(r_{k,\mathbf{x}_\tau}^{vj}, \theta_{\mathrm{t},i}^s\right)}\right)\right], \quad (39)$$

where (a) is from the CDF of the Gamma distribution, and (b) follows from the definition of the incomplete gamma function for integer values of m_v. From (39), we obtain (24) by using $\mathbb{E}_{I^s}[\exp(-z(I^s + \sigma^2))] = \mathcal{L}_{I^s}(z)\exp(-z\sigma^2)$ and following property

$$\mathbb{E}_{I^s}[(-I^s)^n \exp(-zI^s)] = \frac{d}{dz^n}\mathcal{L}_{I^s}(z). \quad (40)$$

In (24), $\mathcal{L}_{I^{\mathrm{IS}}}(z) = \mathcal{L}_{I_0^{\mathrm{IS}}}(z)$ and $\mathcal{L}_{I^{\mathrm{ES}}}(z) = \mathcal{L}_{I_{\mathrm{G}}^{\mathrm{ES}}}(z)\mathcal{L}_{I_{\mathrm{A}}^{\mathrm{ES}}}(z)$, and $\mathcal{L}_{I_l^s}(z)$ is given by

$$\mathcal{L}_{I_l^s}(z) = \mathbb{E}_{\Phi_{\mathrm{I},l}}\left[\exp\left(-z\sum_{\mathbf{x}\in\Phi_{\mathrm{I},l}\backslash\{\mathbf{x}_\tau\}} P_{\mathrm{t}}\Omega_{k,\mathbf{x}} l_v(r_{k,\mathbf{x}}) G_j(r_{k,\mathbf{x}}, \theta_{\mathrm{t},l}^s)\right)\right]$$

$$= \mathbb{E}_{\Phi_{\mathrm{I},l}}\left[\prod_{\mathbf{x}\in\Phi_{\mathrm{I},l}\backslash\{\mathbf{x}_\tau\}} \mathbb{E}_{\Omega_{k,\mathbf{x}}}\left[\exp\left\{-zP_{\mathrm{t}}\Omega_{k,\mathbf{x}} l_v(r_{k,\mathbf{x}}) G_j(r_{k,\mathbf{x}}, \theta_{\mathrm{t},l}^s)\right\}\right]\right]$$

$$\overset{(a)}{=} \mathbb{E}_{\Phi_{\mathrm{I},l}}\left[\prod_{\mathbf{x}\in\Phi_{\mathrm{I},l}\backslash\{\mathbf{x}_\tau\}}\left\{\frac{p_{\mathrm{L}}(r_{k,\mathbf{x}})}{\left(1 + \frac{z}{m_{\mathrm{L}}}P_{\mathrm{t}}l_{\mathrm{L}}(r_{k,\mathbf{x}}) G_j(r_{k,\mathbf{x}}, \theta_{\mathrm{t},l}^s)\right)^{m_{\mathrm{L}}}}\right.\right.$$

$$\left.\left.+ \frac{p_{\mathrm{N}}(r_{k,\mathbf{x}})}{1 + zP_{\mathrm{t}}l_{\mathrm{N}}(r_{k,\mathbf{x}}) G_j(r_{k,\mathbf{x}}, \theta_{\mathrm{t},l}^s)}\right\}\right], \quad (41)$$

where $\mathbf{x}_\tau$ is the location of the serving BS, and (a) is from the Laplace transforms of the Gamma distribution and the exponential distribution. From (41), by applying the probability generating functional (PGFL) [42], we obtain (25). By averaging $\mathcal{P}_{\mathrm{o},j}^v(r_{k,\mathbf{x}_\tau}^{vj}, \theta_{\mathrm{t},i}^s)$ over $r_{k,\mathbf{x}_\tau}^{vj}$, $\mathcal{P}_{\mathrm{no},i}^s(\theta_{\mathrm{t},i}^s)$ in (38) is obtained as

$$\mathcal{P}_{\mathrm{no},i}^s(\theta_{\mathrm{t},i}^s) = \mathbb{E}_{r_{k,\mathbf{x}_\tau}^{vj}}\left[\mathcal{P}_{\mathrm{o},j}^v(r_{k,\mathbf{x}_\tau}^{vj}, \theta_{\mathrm{t},i}^s)\right]$$

$$\overset{(a)}{=} \sum_{\substack{v\in\{\mathrm{L,N}\},\\ j\in\{1,2,3\}}}\left(\int_{b_{k,j}(\theta_{\mathrm{t},i}^s)}^{b_{k,j+1}(\theta_{\mathrm{t},i}^s)} \mathcal{A}_{vj}^a \mathcal{P}_{\mathrm{o},j}^v(r, \theta_{\mathrm{t},i}^s) f_{r_{k,\mathbf{x}_\tau}^{vj}}^{s,a}(r)dr\right), \quad (42)$$

where (a) is from the definition of $\Phi_{\mathrm{B},l}^{vj}$ in (12). In (42) $f_{r_{k,\mathbf{x}_\tau}^{vj}}^{s,a}(r) = f_{r_i^{vj}}^{s,a}(r)$, and $b_{k,j}(\theta_{\mathrm{t},i}^s) = b_{i,j}(\theta_{\mathrm{t},i}^s)$ as $k \in \mathcal{U}_i$. By substituting (42) into (38), we obtain (23).

REFERENCES

[1] S. Kim, M. Kim, J. Y. Ryu, and J. lee, "Impact of base station antenna tilt angle on UAV communications," in *Proc. IEEE Global Commun. Conf. (GLOBECOM)*, Taipei, Taiwan, Dec. 2020, pp. 1–6.

[2] F. Rinaldi, H.-L. Maattanen, J. Torsner, S. Pizzi, S. Andreev, A. Iera, Y. Koucheryavy, and G. Araniti, "Non-terrestrial networks in 5G & beyond: A survey," *IEEE Access*, vol. 8, pp. 165 178–165 200, Sep. 2020.

[3] M. Giordani and M. Zorzi, "Non-terrestrial networks in the 6G era: Challenges and opportunities," *IEEE Netw.*, vol. 35, no. 2, pp. 244–251, Mar. 2021.

[4] X. Lin, S. Rommer, S. Euler, E. A. Yavuz, and R. S. Karlsson, "5G from space: An overview of 3GPP non-terrestrial networks," *arXiv*, Mar. 2021. [Online]. Available: https://arxiv.org/abs/2103.09156

[5] Y. Zeng, R. Zhang, and T. J. Lim, "Wireless communications with unmanned aerial vehicles: opportunities and challenges," *IEEE Commun. Mag.*, vol. 54, no. 5, pp. 36–42, May 2016.

[6] N. H. Motlagh, M. Bagaa, and T. Taleb, "UAV-based IoT platform: A crowd surveillance use case," *IEEE Commun. Mag.*, vol. 55, no. 2, pp. 128–134, Feb. 2017.

[7] S. Hayat, E. Yanmaz, and R. Muzaffar, "Survey on unmanned aerial vehicle networks for civil application: A communications viewpoint," *IEEE Commun. Surveys Tuts.*, vol. 18, no. 4, pp. 2624–2661, Fourth Quart. 2016.

[8] A. A. Khuwaja, Y. Chen, N. Zhao, M. Alouini, and P. Dobbins, "A survey of channel modeling for UAV communications," *IEEE Commun. Surveys Tuts.*, vol. 20, no. 4, pp. 2804–2821, Fourth Quart. 2018.

[9] A. Al-Hourani and K. Gomez, "Modeling cellular-to-UAV path-loss for suburban environments," *IEEE Wireless Commun. Lett.*, vol. 7, no. 1, pp. 82–85, Feb. 2018.

[10] A. Al-Hourani, S. Kandeepan, and S. Lardner, "Optimal LAP altitude for maximum coverage," *IEEE Wireless Commun. Lett.*, vol. 3, no. 6, pp. 569–572, Dec. 2014.

[11] H. Cho, C. Liu, J. Lee, T. Noh, and T. Q. S. Quek, "Impact of elevated base stations on the ultra-dense networks," *IEEE Commun. Lett.*, vol. 22, no. 6, pp. 1268–1271, Jun. 2018.

[12] M. M. Azari, F. Rosas, K. Chen, and S. Pollin, "Ultra reliable UAV communication using altitude and cooperation diversity," *IEEE Trans. Commun.*, vol. 66, no. 1, pp. 330–344, Jan. 2018.

[13] P. K. Sharma and D. I. Kim, "UAV-enabled downlink wireless system with non-orthogonal multiple access," in *Proc. IEEE Global Commun. Conf. Workshops. (GC Wkshps)*, Singapore, Dec. 2017, pp. 1–6.

[14] H. He, S. Zhang, Y. Zeng, and R. Zhang, "Joint altitude and beamwidth optimization for UAV-enabled multiuser communications," *IEEE Commun. Lett.*, vol. 22, no. 2, pp. 344–347, Feb. 2018.

[15] M. Mozaffari, W. Saad, M. Bennis, and M. Debbah, "Efficient deployment of multiple unmanned aerial vehicles for optimal wireless coverage," *IEEE Commun. Lett.*, vol. 20, no. 8, pp. 1647–1650, Aug. 2016.

[16] J. Lyu, Y. Zeng, and R. Zhang, "UAV-aided offloading for cellular hotspot," *IEEE Trans. Wireless Commun.*, vol. 17, no. 6, pp. 3988–4001, Jun. 2018.

[17] S. Zhang, Y. Zeng, and R. Zhang, "Cellular-enabled UAV communication: A connectivity-constrained trajectory optimization perspective," *IEEE Trans. Commun.*, vol. 67, no. 3, pp. 2580–2604, Mar. 2019.

[18] M. Kim and J. Lee, "Impact of an interfering node on unmanned aerial vehicle communications," *IEEE Trans. Veh. Technol.*, vol. 68, no. 12, pp. 12 150–12 163, Dec. 2019.

[19] D. Kim, J. Lee, and T. Q. S. Quek, "Multi-layer unmanned aerial vehicle networks: Modeling and performance analysis," *IEEE Trans. Wireless Commun.*, vol. 19, no. 1, pp. 325–339, Jan. 2020.

[20] Y. Zeng, J. Lyu, and R. Zhang, "Cellular-connected UAV: Potential, challenges, and promising technologies," *IEEE Wireless Commun.*, vol. 26, no. 1, pp. 120–127, Feb. 2019.

[21] X. Lin, V. Yajnanarayana, S. D. Muruganathan, S. Gao, H. Asplund, H. Maattanen, M. Bergstrom, S. Euler, and Y. . E. Wang, "The sky is not the limit: LTE for unmanned aerial vehicles," *IEEE Commun. Mag.*, vol. 56, no. 4, pp. 204–210, Apr. 2018.

[22] B. Galkin, J. Kibilda, and L. A. DaSilva, "Backhaul for low-altitude UAVs in urban environments," in *Proc. IEEE Int. Conf. Commun. (ICC)*, Kansas City, MO, May 2018, pp. 1–6.

[23] M. M. Azari, F. Rosas, A. Chiumento, and S. Pollin, "Coexistence of terrestrial and aerial users in cellular networks," in *Proc. IEEE Global Commun. Conf. Workshops. (GC Wkshps)*, Singapore, Dec. 2017, pp. 1–6.

[24] M. M. Azari, F. Rosas, and S. Pollin, "Reshaping cellular networks for the sky: Major factors and feasibility," in *Proc. IEEE Int. Conf. Commun. (ICC)*, Kansas City, MO, May 2018, pp. 1–7.

[25] R. Amer, W. Saad, and N. Marchetti, "Toward a connected sky: Performance of beamforming with down-tilted antennas for ground and UAV user co-existence," *IEEE Commun. Lett.*, vol. 23, no. 10, pp. 1840–1844, Oct. 2019.

[26] X. Xu and Y. Zeng, "Cellular-connected UAV: Performance analysis with 3D antenna modeling," in *Proc. IEEE Int. Conf. Commun. Workshops. (ICC Wkshps)*, Shanghai, China, May 2019, pp. 1–6.

[27] R. Amer, W. Saad, B. Galkin, and N. Marchetti, "Performance analysis of mobile cellular-connected drones under practical antenna configurations," in *Proc. IEEE Int. Conf. Commun. (ICC)*, Dublin, Ireland, Jun. 2020, pp. 1–7.

[28] R. Amer, W. Saad, and N. Marchetti, "Mobility in the sky: Performance and mobility analysis for cellular-connected UAVs," *IEEE Trans. Commun.*, vol. 68, no. 5, pp. 3229–3246, May 2020.

[29] 3rd Generation Partnership Project, "Technical specification group radio access network; evolved universal terrestrial radio access (E-UTRA); further advancements for E-UTRA physical layer aspects," TR 36.814 V9.2.0, Tech. Rep., Mar. 2017, release 9.

[30] Y. Zhu, G. Zheng, and M. Fitch, "Secrecy rate analysis of uav-enabled mmwave networks using matérn hardcore point processes," *IEEE J. Sel. Areas Commun.*, vol. 36, no. 7, pp. 1397–1409, Jul. 2018.

[31] J. Lyu and H.-M. Wang, "Secure uav random networks with minimum safety distance," *IEEE Trans. Veh. Technol.*, vol. 70, no. 3, pp. 2856–2861, Mar. 2021.

[32] Z. Yang, L. Zhou, G. Zhao, and S. Zhou, "Blockage modeling for inter-layer UAVs communications in urban environments," in *Proc. IEEE Int. Conf. Telecommun. (ICT)*, St. Malo, France, Jun. 2018, pp. 307–311.

[33] R. Hernandez-Aquino, S. A. R. Zaidi, D. McLernon, M. Ghogho, and A. Imran, "Tilt angle optimization in two-tier cellular networks—a stochastic geometry approach," *IEEE Trans. Commun.*, vol. 63, no. 12, pp. 5162–5177, Dec. 2015.

[34] S. M. Razavizadeh, M. Ahn, and I. Lee, "Three-dimensional beamforming: A new enabling technology for 5g wireless networks," *IEEE Signal Process. Mag.*, vol. 31, no. 6, pp. 94–101, Nov. 2014.

[35] M. Alzenad and H. Yanikomeroglu, "Coverage and rate analysis for unmanned aerial vehicle base stations with LoS/NLoS propagation," in *Proc. IEEE Global Commun. Conf. Workshops. (GC Wkshps)*, Abu Dhabi, UAE, Dec. 2018, pp. 1–7.

[36] F. Baccelli and B. Błaszczyszyn, *Stochastic Geometry and Wireless Networks, Volume II — Applications*, ser. Foundations and Trends in Networking. NoW Publishers, 2009.

[37] H. ElSawy, A. Sultan-Salem, M. Alouini, and M. Z. Win, "Modeling and analysis of cellular networks using stochastic geometry: A tutorial," *IEEE Commun. Surveys Tuts.*, vol. 19, no. 1, pp. 167–203, First Quart. 2017.

[38] S. S. Ikki and M. H. Ahmed, "Performance analysis of decode-and-forward incremental relaying cooperative-diversity networks over rayleigh fading channels," in *Proc. IEEE Veh. Technol. Conf. (VTC)*, Barcelona, Spain, Apr. 2009, pp. 1–6.

[39] I. S. Gradshteyn and I. M. Ryzhik, *Table of Integrals, Series, and Products*, 7th ed. San Diego, CA, USA: Academic Press, 2007.

[40] 3rd Generation Partnership Project, "Technical specification group radio access network; study on enhanced lte support for aerial vehicles," TR 36.777 V15.0.0, Tech. Rep., Dec. 2017, release 15.

[41] J. Holis and P. Pechac, "Elevation dependent shadowing model for mobile communications via high altitude platforms in built-up areas," *IEEE Trans. Antennas Propag.*, vol. 56, no. 4, pp. 1078–1084, Apr. 2008.

[42] M. Haenggi and R. K. Ganti, "Interference in large wireless networks," *Foundations and Trends in Networking*, vol. 3, no. 2, pp. 127–248, 2009.